

Master Thesis

Non-intrusive impedance measurement techniques: models and sensitivity analysis

Author

Pablo López Callejo

Supervised by

Flavio Canavero

Igor Simone Stievano



Dipartimento di Elettronica e delle Telecomunicazioni

Politecnico di Torino

Torino, Italy

March 2022

Non-intrusive impedance measurement techniques: models and sensitivity analysis

Pablo López Callejo

Supervised by:

Flavio Canavero

Stievano Igor Simone

Dipartimento di Elettronica e Telecomunicazioni

Abstract

Among the diverse techniques developed for in-circuit impedance measuring some of the most studied ones nowadays are those which are non-intrusive, that is, they are not electrically connected to the current of the circuit under test. In particular, one of the most popular methods is the so-called *two-probes set-up measurement method* which has been notably used in a number of applications. The aim of this work is to compare, in terms of robustness against measurement errors, this well-established method to one that has been developed recently and which uses only one probe: the *single-probe method*.

To carry out this comparison two types of analysis have been conducted: a *Montecarlo analysis*, which consists in performing a high number of simulations slightly randomly changing the parameter values of the test set-up that are used for impedance estimation; and a *sensitivity analysis*, whose goal is to quantify which parameters have a larger impact in the final estimate. By performing these analyses it can be seen which method has a larger robustness against an error in each one of the parameters as well as the frequencies which turn out to be most critical.

Also, as the single-probe method is a relatively new one, several simulations using diverse softwares have been conducted to test its performance, placing two different scenarios: one in which the device under test is a passive ideal circuit (only the impedance to be measured) and another one fed by a DC voltage and in which the losses in wire have been considered.

The final outcome of this work is that the single probe method turns out to exhibit a larger parameter sensitivity effect in a frequency range close to a resonant behaviour of the impedance under test. However, it offers a viable yet simpler alternative which can be effectively used in practical applications. Also, the mentioned larger sensitivity can be overcome by a more precise characterization of the critical parameters.

Contents

1	Introduction	11
1.1	Motivations	12
1.2	Goals	12
2	Generalities and State of the Art	13
2.1	Background theory	13
2.1.1	AC analysis	13
2.1.2	Two-port network theory	14
2.2	Impedance measurement techniques	21
2.2.1	Intrusive methods	22
2.2.1.1	I-V approach	23
2.2.1.2	Capacitive coupling approach	24
2.2.2	Non-intrusive methods	25
2.2.3	Inductive probes	26
3	Methodology	27
3.1	Passive ideal DUT	28
3.2	DUT with supply and losses in wire	30
3.3	Two-probes set-up	31
3.4	LTSpice implementation of the test set-up	33
4	Development of the Work	35
4.1	Parameters and data	35
4.2	Matlab simulations	37
4.2.1	Ideal passive DUT circuit	37
4.2.2	DUT with losses in wire and DC supply	38
4.3	LTSpice and Matlab simulations	39
4.4	Qucs and Matlab simulations	40
4.4.1	Ideal passive DUT	40
4.4.2	DUT with losses in wire and DC supply	41
4.5	Montecarlo and sensitivity analysis	43
4.5.1	Notation	43
4.5.2	Montecarlo analysis	45
4.5.2.1	Ideal passive DUT	45
4.5.2.2	DUT with wire losses and DC supply	46
4.5.2.3	Two-probes set-up	47
4.5.3	Sensitivity analysis	48
4.5.3.1	Ideal passive DUT	49
4.5.3.2	DUT with losses in wire and DC supply	51

4.5.3.3	Two-probes set-up	54
5	Remarks and conclusions	56
5.1	Outcome discussion	56
5.1.1	Simulations results	56
5.1.2	Montecarlo analysis results	56
5.1.3	Sensitivity analysis results	57
5.2	Conclusions	57
5.3	Future works	58

List of Figures

2.1	Bode plot example	14
2.2	Two-port network	14
2.3	T-network	15
2.4	Π -network	16
2.5	Two-port network connections (1)	19
2.6	Two-port network connections (2)	20
2.7	Several intrusive impedance measure techniques	22
2.8	I-V method	23
2.9	I-V method in high frequencies	23
2.10	I-V method with energized DUT	24
2.11	Capacitive coupling method with energized DUT	24
2.12	Capacitive coupling approach for impedance spectroscopy	25
2.13	inductive probe example	26
3.1	DUT and probe set-up	27
3.2	DUT and probe set-up	28
3.3	Pre-characterization 1	28
3.4	Pre-characterization 2	30
3.5	Two-probe set-up schematic	31
3.6	Two-probe set-up model	32
3.7	Representation as coupled coils	33
3.8	Representation as ideal transformer	34
4.1	RLC Load	35
4.2	Data digitization comparative	36
4.3	Matlab simulation of ideal DUT	37
4.4	Schematic of active DUT with wire losses	38
4.5	Matlab simulation of active DUT with wire losses	38
4.6	LTspice netlist (transformer representation of the probe)	39
4.7	LTspice simulation (transformer representation of the probe)	39
4.8	Qucs schematics for ideal DUT simulation	40
4.9	Qucs ideal DUT simulation output	41
4.10	Qucs schematics for DUT with DC supply and losses in wire simulation	42
4.11	Qucs DUT with DC supply and losses in wire simulation output	42
4.12	Montecarlo analysis passive ideal DUT	45
4.13	Montecarlo analysis of DUT with DC supply and losses in wire	46
4.14	Montecarlo analysis with the two-probes set-up	47
4.15	example of a simple function elasticity	48
4.16	Sensitivity analysis passive ideal DUT	50

4.17	Sensitivity analysis DUT with cable and supply (part 1)	51
4.18	Sensitivity analysis DUT with cable and supply (part 2)	52
4.19	Sensitivity analysis DUT with cable and supply (part 3)	53
4.20	Sensitivity analysis with two-probes set-up (part 1)	54
4.21	Sensitivity analysis with two-probes set-up (part 2)	55

Chapter 1

Introduction

Impedance measurement has a lot of practical applications in both technical and research fields. The cases in which this practice is used include electromagnetic properties measurement of materials, sensor reading, semiconductor characterization, electrical devices health monitoring and even medical or biological applications [3]. In the last decades the circuit impedance measurement techniques have been being developed to be performed in already working electrical systems with the aim of getting data of the current state of the system or device. As an example, online measuring the impedance of a lithium battery allows to know its state of charge, state of health and internal temperature [5]. Also important applications of these techniques can be found when working with switched-mode power supplies (SMPS) and designing electromagnetic interference filters (EMI) [12].

Techniques for impedance measuring are diverse and they can be classified attending the way connections with the circuit are made:

- **Intrusive methods:** they imply an electrical connection to the current of the device under test (DUT) as, for example, a capacitive coupling.
- **Non-intrusive methods:** they are attached without an electrical direct connection to the current of the DUT, using for it devices like inductive probes.

All of this work is focused on these last kind of methods, however, the first ones will also be briefly reviewed.

Among all non-intrusive methods it can be remarked the *two-probe set-up* method, whose importance has been growing in the last years and has been used in several articles [4]. This technique consist in clamping two inductive probes to the DUT and connect them to a two-port VNA. For each port a frequency swept is performed and the S-parameters of the whole system are obtained [16]. Then with this values and the correspondent S-parameters of both of the probes (that have been previously characterized), the value of the impedance is computed following the method explained in section 3.3.

However, this well-established method have shown certain weaknesses as for example an undesirable inductive coupling among the probes [15]. Therefore, another method using only one probe has been developed recently, which not only address this probe-to-probe coupling problem, but also can be performed with time-domain-based instrumentation, which is useful for impedance monitoring.

When performed with frequency-domain-based instrumentation such as an impedance analyser, this technique is carried out by taking four different impedance measurements at the probe input, each one with a different loads: one with the actual load whose unknown impedance value is the target to be computed, and three already known impedances. With these four measurements and the values of the known impedance used, the target impedance value is computed by applying the formulas explained in sections 3.1 and 3.2. This single-probe set-up method with frequency-domain-based instrumentation is the case on which this work has focused.

1.1 Motivations

The single-probe method has been developed to address some of the weaknesses that the two-probes method has shown, as for example the probe characterization error propagation or the previously mentioned inductive coupling among the probes [16]. Even although a calibration error has been developed for the two-probes set-up these errors persist [18], therefore, the single-probe approach could gain importance. Consequently, compare the advantage and disadvantages of this relatively new method against the already established one can be really useful for the field and practices in which the in-circuit impedance measurement is required, and this is the motivation of this work.

1.2 Goals

The goals of this work are essentially two:

- To assess the single-probe method performance through simulations using several diverse software and scenarios, with the aim to verify its correct working and the accuracy of the outcome through diverse representations.
- To compare this new method to the two-probes set-up technique in terms of theoretical robustness against measurement errors, conducting to this purpose two different analysis, called *Montecarlo analysis* and *sensitivity analysis*. These analysis are explained in detail in section 4.5 and are useful to see how much the outcomes of the two techniques vary when the parameters of the methods are modified.

Chapter 2

Generalities and State of the Art

2.1 Background theory

Through this section the basic mathematical tools used in this work are explained. Those are the frequency-domain analysis and the two-port networks theory.

2.1.1 AC analysis

In this work all the simulation, analysis and graphics are conceived in the scope of the frequency domain, that is, the components and circuits are analysed by doing a swept in the values of the frequency. This is useful to analyse the response of components and circuits that work under alternating current (AC), that is, a sinusoidal signal. When the circuits considered have only a single frequency, the phasorial notation can be used, for example a sinusoidal voltage with amplitude V (V), frequency ω (rad/s) and phase ψ (rad) would be represented as:

$$\begin{aligned} V \cos(\omega t + \psi) &= \operatorname{Re}(V \cos(\omega t + \psi) + jV \cos(\omega t + \psi)) = \\ &= \operatorname{Re}(V e^{j(\omega t + \psi)}) = \operatorname{Re}(V e^{j\omega t} e^{j\psi}) = \operatorname{Re}(e^{j\omega t} \underline{V}) \end{aligned}$$

where t is the time in seconds and j the imaginary unit. As the factor $e^{j\omega t}$ is the same for all the electrical variables when considering a single frequency in the system, the voltage can be fully represented by \underline{V} which is call *phasor* and have several notations:

$$\underline{V} = V e^{j\psi} := V \angle \psi$$

When using this representation the mathematical operations that are used in direct current can be used in AC considering the complex algebra. Therefore, the complex impedance is defined as:

$$\underline{Z} = \frac{\underline{V}}{\underline{I}} = \frac{V}{I} \angle \psi_V - \psi_I$$

where V and I are the magnitudes of voltage and current and ψ_V and ψ_I the phases respectively.

As stated previously, by doing a frequency swept in a certain range of values the behaviour of components and circuits can be studied. Usually the data obtained from this type of analysis is presented through graphics like the Bode plot. This sort of graphics shows the frequency response of a system, that is the gain (defined as the ratio between the output and the input of the variable considered) against frequency, for both magnitude and phase and uses logarithmic scales. An example of these kind of graphics can be found in figure 2.1.

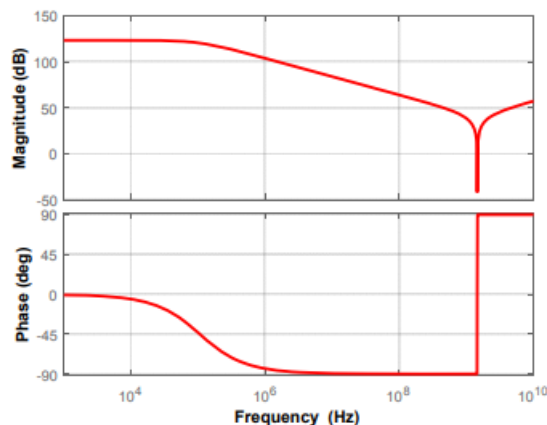


Figure 2.1: Bode plot example extracted from [2]

2.1.2 Two-port network theory

When the system analysed has a certain grade of complexity it is convenient to considerate it as different encapsulated networks and compute the voltages and currents in their connections. This terminal connections of each network are called *ports* and can be several for each network depending on the topology of the system but through this subsection only the ones with two ports are explained, as they are the only ones used in this work. Also for this whole subsection the circuits that constitute the networks are supposed to be lineal.

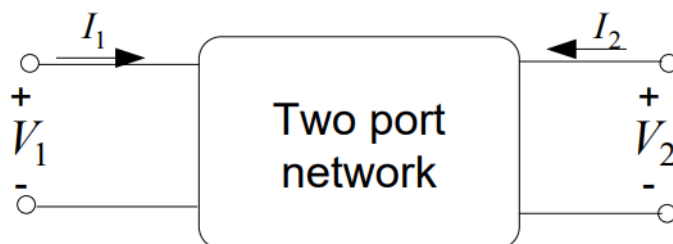


Figure 2.2: Schematic of a two-port network with sign criteria, extracted from [1]

In figure 2.2 the schematic of a two-port network can be seen. The relation between V_1 , I_1 , V_2 and I_2 can be determined by the parameters of the network, that are obviously dependent from the network inner configuration. There are a lot of ways to define this parameters, the most used are explained next.

Z-parameters

They are also called impedance parameters because they are defined by the ratios among the ports voltages and currents respectively. The parameters and their correspondent matrix \mathbf{Z} are the defined as it follows:

$$\begin{pmatrix} V_1 \\ V_2 \end{pmatrix} = \begin{pmatrix} z_{11} & z_{12} \\ z_{21} & z_{22} \end{pmatrix} \begin{pmatrix} I_1 \\ I_2 \end{pmatrix} = \mathbf{Z} \begin{pmatrix} I_1 \\ I_2 \end{pmatrix}$$

where

$$z_{11} = \left. \frac{V_1}{I_1} \right|_{I_2=0} \quad z_{12} = \left. \frac{V_1}{I_2} \right|_{I_1=0}$$

$$z_{21} = \left. \frac{V_2}{I_1} \right|_{I_2=0} \quad z_{22} = \left. \frac{V_2}{I_2} \right|_{I_1=0}$$

When matrix \mathbf{Z} is symmetric the network is called *reciprocal* and when $z_{11} = z_{22}$ is called *symmetrical*. Z-parameters also have a direct conversion formula into a T-network, as shown in figure 2.4.

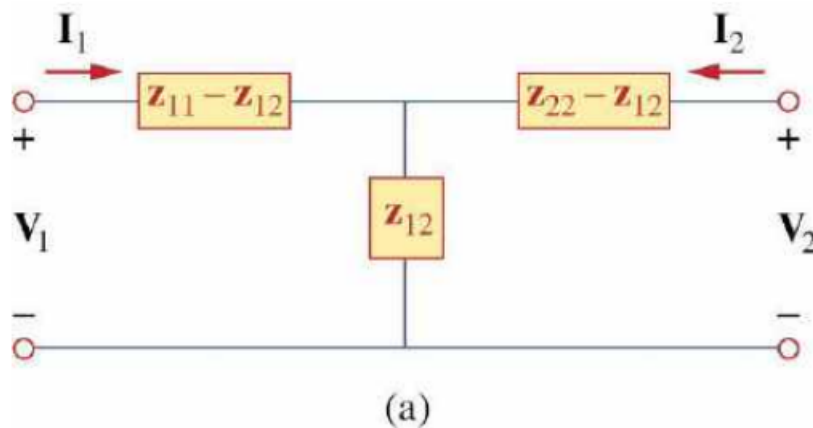


Figure 2.3: Relation between T-network impedances and Z-parameters, extracted from [1]

Y-parameters

Also known as admittance parameters because, contrary to the Z-parameters, the ports currents are defined linearly in terms of the ports voltages. The parameters and their correspondent matrix \mathbf{Y} are the defined as it follows:

$$\begin{pmatrix} I_1 \\ I_2 \end{pmatrix} = \begin{pmatrix} y_{11} & y_{12} \\ y_{21} & y_{22} \end{pmatrix} \begin{pmatrix} V_1 \\ V_2 \end{pmatrix} = \mathbf{Y} \begin{pmatrix} V_1 \\ V_2 \end{pmatrix}$$

where

$$y_{11} = \left. \frac{I_1}{V_1} \right|_{V_2=0} \quad y_{12} = \left. \frac{I_1}{V_2} \right|_{V_1=0}$$

$$y_{21} = \left. \frac{I_2}{V_1} \right|_{V_2=0} \quad y_{22} = \left. \frac{I_2}{V_2} \right|_{V_1=0}$$

When matrix \mathbf{Y} is symmetric the network is called *reciprocal* and when $y_{11} = y_{22}$ is called *symmetrical*. Z-parameters also have a direct conversion formula into a Π -network, as shown in figure 2.4.

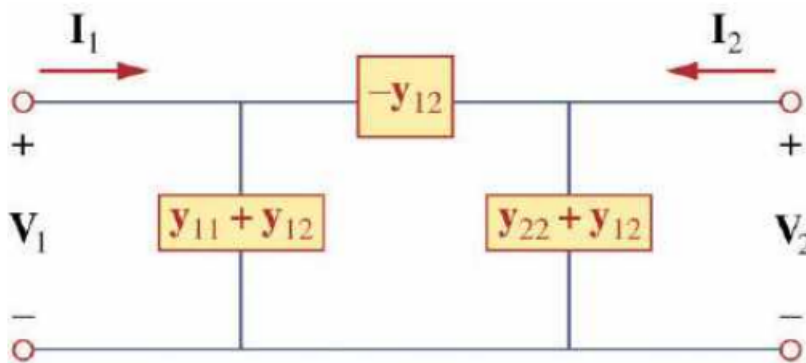


Figure 2.4: Relation between Π -network admittances and Y-parameters, extracted from [1]

H-parameters

They are also called hybrid parameters and they are obtained when current at port 1 and voltage at port 2 are considered the independent variables. The parameters and their correspondent matrix \mathbf{H} are the defined as it follows:

$$\begin{pmatrix} V_1 \\ I_2 \end{pmatrix} = \begin{pmatrix} h_{11} & h_{12} \\ h_{21} & h_{22} \end{pmatrix} \begin{pmatrix} I_1 \\ V_2 \end{pmatrix} = \mathbf{H} \begin{pmatrix} I_1 \\ V_2 \end{pmatrix}$$

where

$$h_{11} = \left. \frac{V_1}{I_1} \right|_{V_2=0} \quad h_{12} = \left. \frac{V_1}{V_2} \right|_{I_1=0}$$

$$h_{21} = \left. \frac{I_2}{I_1} \right|_{V_2=0} \quad h_{22} = \left. \frac{I_2}{V_2} \right|_{I_1=0}$$

When $h_{12} = -h_{21}$ the network is said to be *reciprocal* and when $\det(\mathbf{H}) = 1$ it is called *symmetrical*.

G-parameters

Also known as hybrid inverse parameters as they are the dual form of the H-parameters. The parameters and their correspondent matrix \mathbf{G} are the defined as it follows:

$$\begin{pmatrix} I_1 \\ V_2 \end{pmatrix} = \begin{pmatrix} g_{11} & g_{12} \\ g_{21} & g_{22} \end{pmatrix} \begin{pmatrix} V_1 \\ I_2 \end{pmatrix} = \mathbf{G} \begin{pmatrix} V_1 \\ I_2 \end{pmatrix}$$

where

$$g_{11} = \left. \frac{I_1}{V_1} \right|_{I_2=0} \quad g_{12} = \left. \frac{I_1}{I_2} \right|_{V_1=0}$$

$$g_{21} = \left. \frac{V_2}{V_1} \right|_{I_2=0} \quad g_{22} = \left. \frac{V_2}{I_2} \right|_{V_1=0}$$

When $g_{12} = -g_{21}$ the network is said to be *reciprocal* and when $\det(\mathbf{G}) = 1$ it is called *symmetrical*.

ABCD-parameters

Also called T-parameters or transmission parameters, obtained when voltage and current of the first port are expressed linearly in terms of the voltage and current of the second port. The parameters and their correspondent matrix \mathbf{T} are the defined as it follows:

$$\begin{pmatrix} V_1 \\ I_1 \end{pmatrix} = \begin{pmatrix} A & B \\ C & D \end{pmatrix} \begin{pmatrix} V_2 \\ -I_2 \end{pmatrix} = \mathbf{T} \begin{pmatrix} V_2 \\ -I_2 \end{pmatrix}$$

where

$$A = \left. \frac{V_1}{V_2} \right|_{I_2=0} \quad B = \left. \frac{V_1}{-I_2} \right|_{V_2=0}$$

$$C = \left. \frac{I_1}{V_2} \right|_{I_2=0} \quad D = \left. \frac{I_1}{-I_2} \right|_{V_2=0}$$

When $\det(\mathbf{T}) = 1$ the network is said to be *reciprocal* and when $A = D$ it is called *symmetrical*. Also their correspondent dual parameters exist and are known as inverse transmission parameters, obtained when voltage and current of the first port are considered as the independent variables instead of ones of the second port.

S-parameters

They are also called scattering parameters and their definition differs from the others explained previously. They are defined using the incident and absorbed waves as variables and are linked to an arbitrary value of impedance in the ports called reference impedance, which is used instead of the short-circuit or open-circuit used to compute the other parameters explained. The S-parameters matrix and equations are the following:

$$\begin{pmatrix} b_1 \\ b_2 \end{pmatrix} = \begin{pmatrix} s_{11} & s_{12} \\ s_{21} & s_{22} \end{pmatrix} \begin{pmatrix} a_1 \\ a_2 \end{pmatrix} = \mathbf{S} \begin{pmatrix} a_1 \\ a_2 \end{pmatrix}$$

where a_1 and a_2 are the incident waves and b_1 and b_2 the reflected waves of ports 1 and 2 of the network, respectively.

Parameters used in this work

All of the parameters previously mentioned have a reason to be defined: each one of them are more suitable depending on the topology of the network connections (except for the scattering parameters, whose reasons are that they are more appropriate for high-frequency measurements and full-wave analysis [6]). In figures 2.5 and 2.6 it can be seen which parameters best fit each configuration.

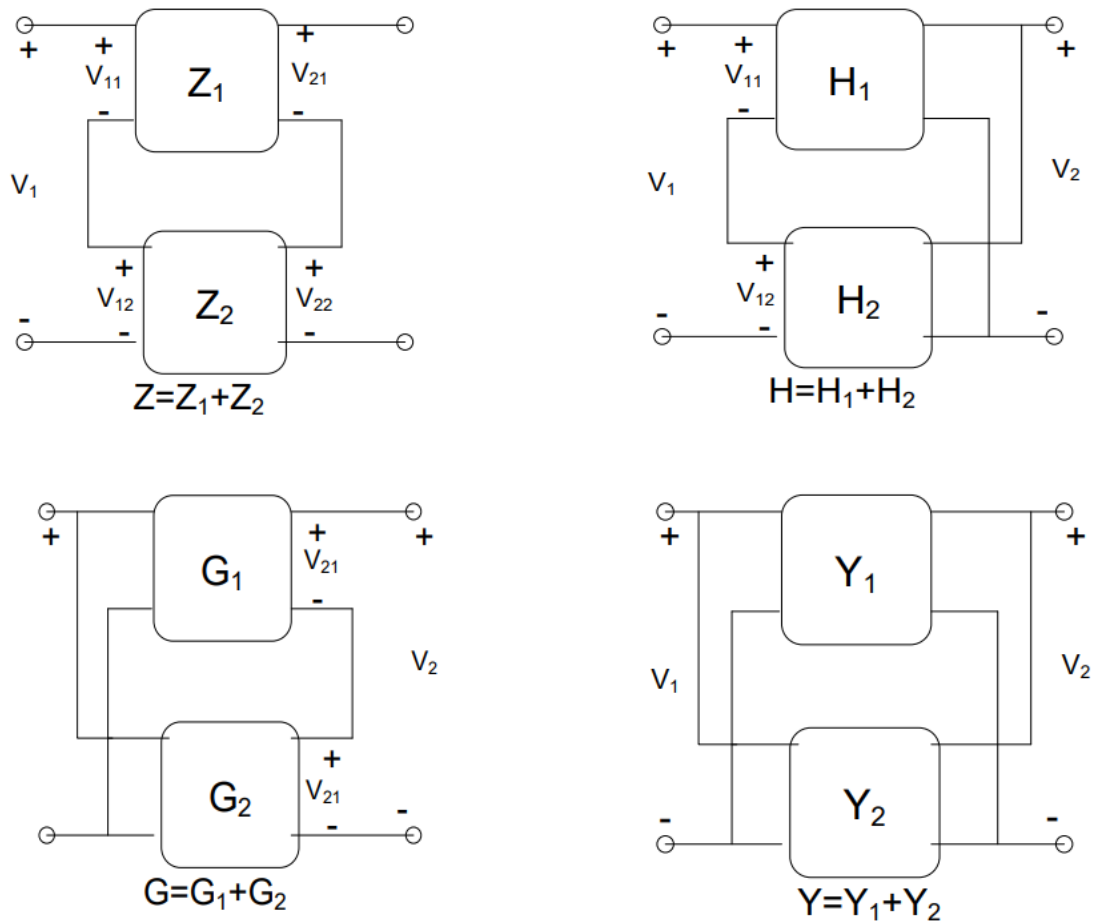


Figure 2.5: Top to bottom and left to right: 1) Series connection implies Z-parameters matrices addition, 2) Series-parallel connection implies H-parameters matrices addition, 3) Parallel-series connection implies G-parameters matrices addition, 4) Parallel connection implies Y-parameters matrices addition. Image extracted from [1]

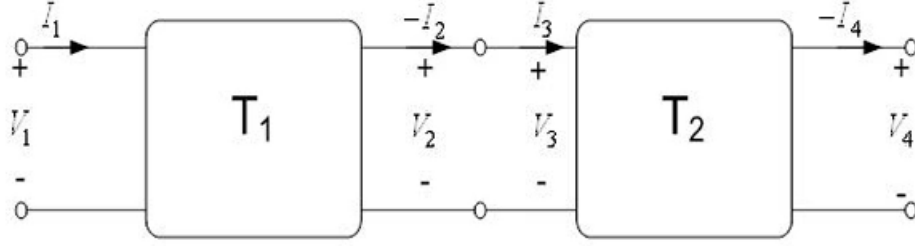


Figure 2.6: Cascade connection implies transmission parameters or inverse transmission parameters matrices multiplication, extracted from [1]

In this work the circuits considered have a cascade topology, therefore ABCD-parameters are used. It has to be mentioned that in this work these parameters are also used in cases in which the network contains independent sources. This implies a modification of the equations mentioned previously: adding an extra term which is a function of the independent source but not of the variables [8]. Then, the ABCD-parameter equations would be the following

$$\begin{pmatrix} V_1 \\ I_1 \end{pmatrix} = \begin{pmatrix} A & B \\ C & D \end{pmatrix} \begin{pmatrix} V_2 \\ -I_2 \end{pmatrix} + \begin{pmatrix} V_{01} \\ I_{01} \end{pmatrix}$$

where

$$V_{01} = V_1 \left| \begin{array}{l} V_2 = 0 \\ I_2 = 0 \end{array} \right. \quad I_{01} = I_1 \left| \begin{array}{l} V_2 = 0 \\ I_2 = 0 \end{array} \right.$$

Also the scattering parameters are used, but only for format purposes in the simulations (Qucs software only admits this representation). The conversion from Z-parameters to S-parameters is directly given by the expression

$$\mathbf{S} = (\mathbf{Z} - \mathbf{Z}_r)(\mathbf{Z} + \mathbf{Z}_r)^{-1}$$

being \mathbf{Z}_r the diagonal matrix with the reference impedances [6]. As in this work the network representation is made through ABCD-parameters, the previous conversion to Z-parameters must be done through the expression

$$\mathbf{Z} = \frac{1}{C} \begin{pmatrix} A & \det(\mathbf{T}) \\ 1 & D \end{pmatrix}$$

2.2 Impedance measurement techniques

There are several ways to classify the diverse impedance measurement techniques that exists nowadays. Attending to the instrumentation used to implement the measure and the way it registers the magnitudes they can be distinguished:

- **Time-domain measurement techniques:** usually performed with TDT/TDR (Time Domain Transmission/Time Domain Reflection) devices. They allows to measure characteristic impedance directly and to locate physical aberrations. OM the other hand their interpretation is more difficult than in the frequency domain and the SNR (Signal-Noise Ratio) obtained are lower [11].
- **Frequency-domain measurement techniques:** most commonly used devices are VNA (Vector Network Analyser) or impedance analysers. They are not able to locate physical aberrations nor to directly measure characteristic impedance but they are easy to interpret and have better SNR [11].

In this work the only type of technique considered for the simulations and analysis is the frequency-domain-based one using an impedance analyser as measurement tool. Also, attending to different criteria the diverse existing impedance measurement methods can be classified as it follows [11]:

- **Direct or indirect techniques:** depending on what is being measured, the impedance targeted itself (direct) or some effect the impedance causes on other magnitudes (indirect). The second type is used normally as a corroboration or when the function measured is more accessible than the impedance.
- **In-circuit or test fixture techniques:** a test fixture is a device designed to host the DUT and and test it with controlled signals, while in in-circuit methods measurements are taken *in-situ* under the DUT normal working conditions. Each one has its advantages and disadvantages but usually it is more accurate to use in-circuit methods due to the possible influence that the test fixture may have on the DUT [11].
- **Intrusive or non-intrusive techniques:** the firsts have an electrical direct connection to the current of the DUT while the seconds not. Non-invasive are usually preferred because they are less likely to interact with and/or distort the DUT electrical signals.

According to these criteria the methods used in these work are classified as indirect, in-circuit, non-intrusive techniques. In the following subsection techniques from both intrusive and non-intrusive are explained.

2.2.1 Intrusive methods

As stated previously, the use of these techniques implies a direct electrical connection to the current of the circuit being tested. Within these category two approaches can be remarked: the I-V method and the capacitive coupling method. Another examples of invasive techniques are shown and briefly explained in figure 2.7.

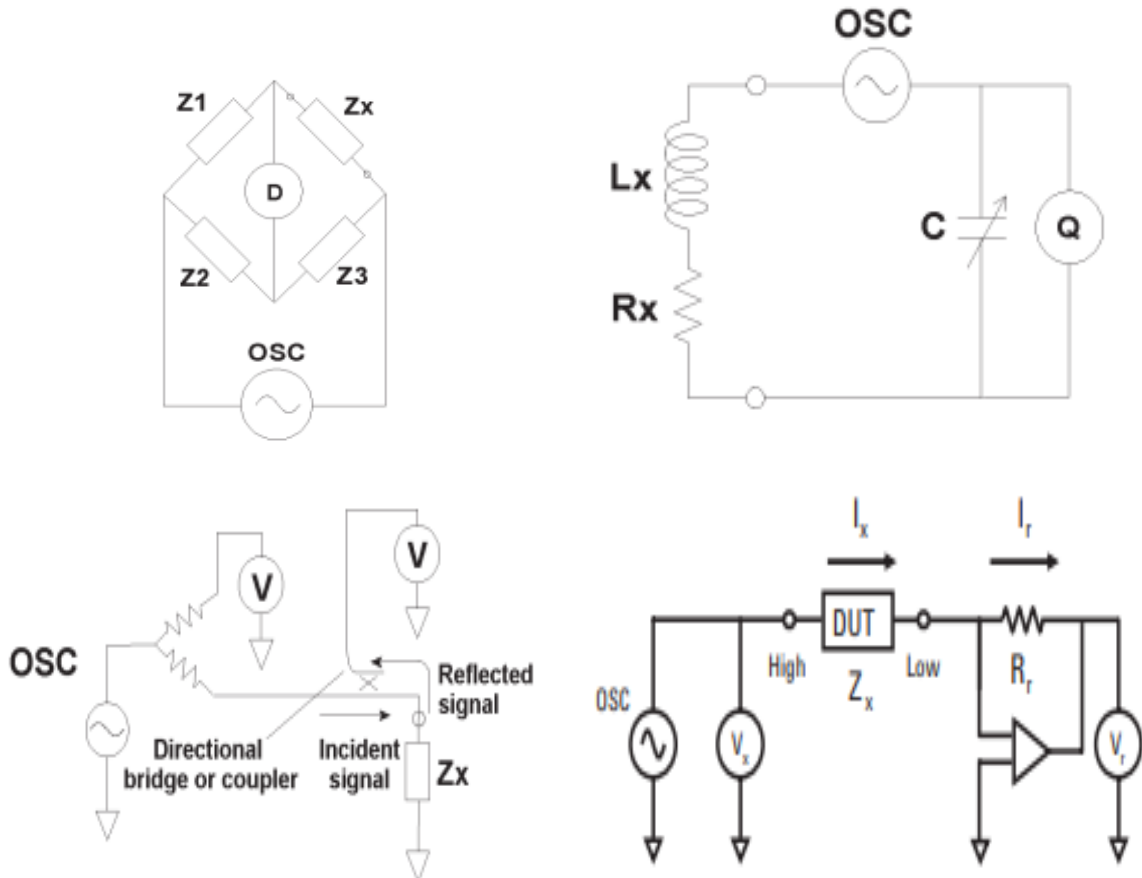


Figure 2.7: Top to bottom and left to right: **1) Bridge method:** when current through D is null the unknown impedance can be computed by $Z_x = \frac{Z_1}{Z_2} Z_3$. **2) Resonant method:** being the circuit previously set in resonance by tuning, L_x and R_x are obtained from C, Q and frequency. **3) Network analysis method:** incident and reflected waves are measured in order to compute the reflection coefficient, which has a direct relation with the unknown impedance. **4) Auto-balancing bridge method:** by creating a virtual ground with the operational amplifier and applying 1st Kirchoff Law unknown impedance is obtained $Z_x = R_r \frac{V_x}{V_r}$. All extracted from [13].

2.2.1.1 I-V approach

This method consists in measure somehow the voltage and current flowing trough the unknown load and compute the impedance value by complex division of the two magnitudes respectively. When the DUT is just a passive load without supply the method implies only taking the measures mentioned before, as seen in figure 2.8, and then applying the formula:

$$\frac{V_1}{R + Z_x} = \frac{V_2}{R} \quad \rightarrow \quad Z_x = R\left(\frac{V_1}{V_2} - 1\right)$$

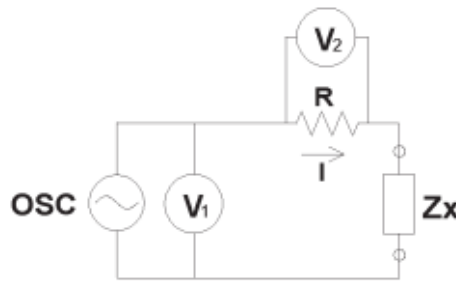


Figure 2.8: Schematic of the I-V method, extracted from [13].

In high frequency scenarios, the set-up is changed to minimize electromagnetic leakage and a coaxial cable is used [13]. Depending on the unknown impedance the measurement circuit configuration differs, as shown in figure 2.9. When the impedance is low it is obtained through:

$$Z_x = \frac{V}{I} = \frac{2V_1}{\frac{V_2}{R} - \frac{V_1}{R}} = \frac{2R}{\frac{V_2}{V_1} - 1}$$

while in case of high impedance:

$$Z_x = \frac{V}{I} = \frac{V_1 - V_2}{\frac{2V_2}{R}} = \frac{R}{2}\left(\frac{V_1}{V_2} - 1\right)$$

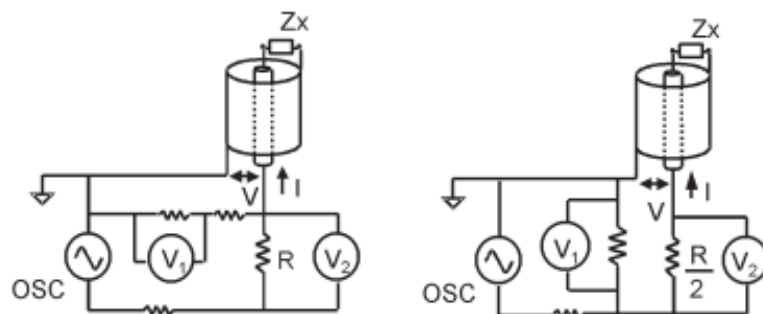


Figure 2.9: Schematic of the I-V method for high frequencies. On the left the low impedance configuration and on the right the correspondent for high impedance. Extracted from [13].

When the DUT is energized (that is, have DC or AC supply) and the load is accessible the procedure shown in figure 2.10 can be followed. In it, the signals obtained from voltage and current are registered in a digital signal processing device to be transformed to the frequency domain and later divided to obtain the complex impedance value.

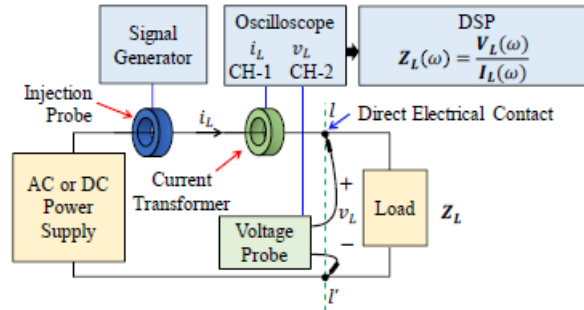


Figure 2.10: Schematic of the I-V method with an energized DUT. In this case the method is being performed with an excitation signal of a known frequency provided by the injection probe, but it can be carried out without it by only measuring voltage and current of a certain frequency. Extracted from [16].

2.2.1.2 Capacitive coupling approach

In this approach the electrical connections with the DUT are implemented through coupling capacitors in parallel connection. This way the high frequency signals used for measure purposes are able to travel through the DUT and these capacitors while the low frequency signals stay in the DUT working normally. In figure 2.11 an example of an energized DUT is shown. The measurement equipment is connected through capacitors C_1 and C_2 , first one is used for injecting an excitation signal and the other for receiving the response. As the signals used for excitation are of high frequencies, two series inductors L_1 and L_2 are needed to avoid the excitation signal propagation to the supply circuit. This way the measurement signal is directed to the targeted impedance [16].

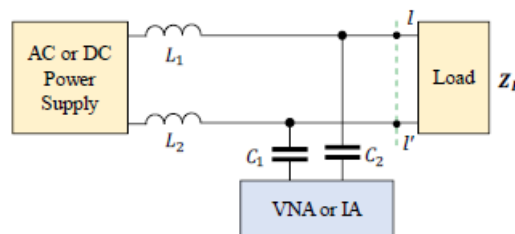


Figure 2.11: Schematic of the capacitive coupling method with an energized DUT. Z_L is the impedance aimed. Extracted from [16].

The value measured at the impedance analyser Z_m is the combination of the impedance from the capacitors, inductors, the source Z_s and the load Z_L . Considering the frequency ω is high then it is obtained:

$$Z_m = \frac{1}{j\omega C_1} + \frac{1}{j\omega C_2} + \frac{(j\omega L_1 + j\omega L_2 + Z_s)Z_L}{j\omega L_1 + j\omega L_2 + Z_s + Z_L} \approx \frac{(j\omega L_1 + j\omega L_2)Z_L}{j\omega L_1 + j\omega L_2} = Z_L$$

The capacitive coupling approach can also be used as a non-intrusive method in impedance spectroscopy activities, particularly when the material targeted has a thin insulating layer at which the electrodes used for measuring are attached [17]. In figure 2.12 the case described is illustrated alongside its equivalent circuit. Similarly to the case in figure 2.11, an excitation signal would be injected through one capacitor and the response would be received through the other to be measured.

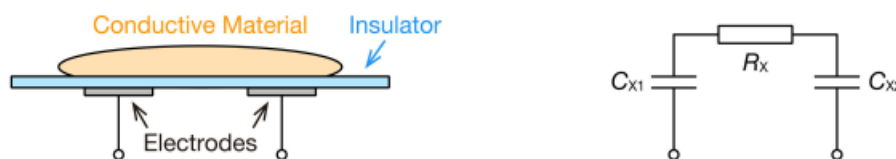


Figure 2.12: Capacitive coupling approach for impedance spectroscopy and equivalent circuit. Extracted from [17].

2.2.2 Non-intrusive methods

As stated previously, non-invasive methods lack in direct electrical contact with the DUT. This implies advantages like a less complex implementation and a lowest electrical hazard for the operating personal and also for the system integrity [15]. Additionally, in cases involving high power feeding the DUT, the devices connecting the measurement equipment to the DUT in intrusive methods like voltage sensors (I-V approach) or coupling capacitors (capacitive coupling approach) can suffer a high dielectric and thermal stresses which may imply their faster degradation and the consequent increase of the maintenance costs, as well as undesirable DUT working stops for replacing [16]. Therefore, non-invasive techniques are usually preferred.

The most common approach is the inductive coupling approach, which uses inductive probes to inject and receive the electrical signals used for the measurements. Typically the number of probes used is two but there exist some applications in which a multi-probe set-up is more suitable, like simultaneous impedances measurement in systems with several branches [16]. The two probes (which are of the clamp-of type) are attached to the wires between the supply system and the load, then using a VNA the S-parameters of the circuit are obtained. Afterwards, with the ABCD-parameters of the probes (previously characterized) along with the ABCD-parameters of the system (obtained from the VNA measurements) the impedance value can be computed. The mathematical model and tools used are explained in section 3.3.

However, it has been recently developed a method using only one probe to achieve the impedance measurement, which has been conceived to avoid the probe-to-probe coupling problems that the two-probe method inevitably suffers [15]. This single-probe method is explained in sections 3.1 and 3.2 and the main goal of this work is to compare it to the two-probe method.

2.2.3 Inductive probes

Inductive probes are widely used in the field of electromagnetic compatibility, for example as a current measurement device to detect sources of radiation or as a signal injector to reproduce coupling effects on wires [10]. They are made of a ferro-magnetic core with a copper wire looped on it (the number of loops depends on the purpose of the probe and the manufacturer). The extremes of this wire are connected to coaxial cable so that it can work as both an input or an output [16]. They are usually designed to be clamped onto the cables, therefore, in this kind of probes the core is split in two. This way, the probe is clamped directly onto the wires of the DUT and interact with it through the magnetic core. In figure 2.13 photographs of an inductive probe are shown.

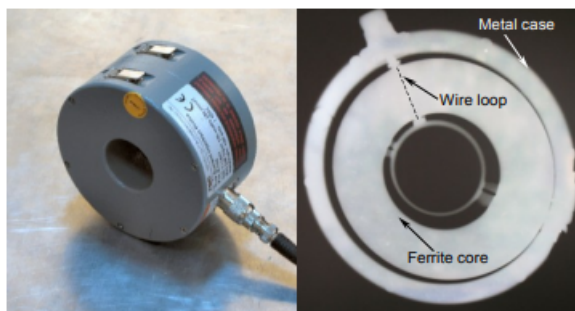


Figure 2.13: Inductive probe example photography and X-ray image (model FCC F-140). Extracted from [9].

Chapter 3

Methodology

Through this chapter the nomenclature and methodology used in this work are explained. The resources and figures as well as the mathematical method itself are all taken from the sections 2.3, 3.1 and 3.2 from [16], except for section 4.5 which is self-developed.

As said in previous chapters, the aim of this work is to try and validate the theoretical robustness and performance of the single-probe impedance measurement method described in [16] against the standard approach, which is the two-probes method. The considered set-up is the one shown in figure 3.1: an active circuit (DUT) with the inductive probe clamped to it and also connected to an impedance analyser device. The DUT has a passive part (the load) whose impedance value has to be estimated (Z_L).

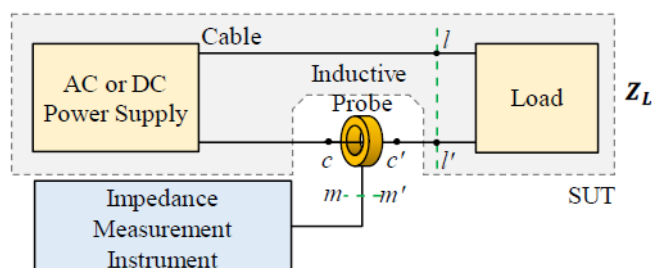


Figure 3.1: Set-up of the single-probe method explained in [16]

Three planes can be defined as shown in the figure 3.1: the $m-m'$ plane between the probe input and the impedance measurement device, the $c-c'$ plane between the DUT and the probe output and the $l-l'$ plane between the the load and the rest of the DUT, that is, the wire and supply. This way this schematic can be rearranged using the two-port circuits theory as shown in figure 3.2, being A_1 , B_1 , C_1 and D_1 the ABCD parameters representation of the inductive probe and A_2 , B_2 , C_2 and D_2 .

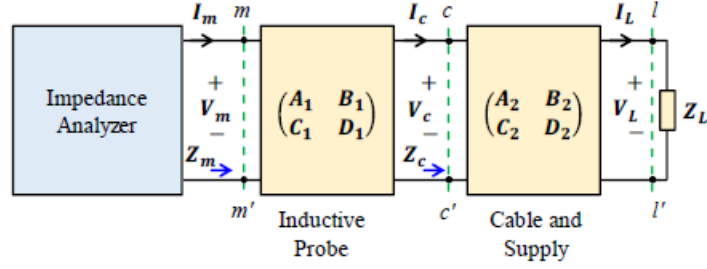


Figure 3.2: Set-up of the single-probe method explained in [16]

To complete the nomenclature explanation, V_k , I_k and Z_k are respectively the voltage, current and impedance seen in the plane k so that $k \in \{m, c, l\}$.

3.1 Passive ideal DUT

In this section the methodology for impedance extraction is addressed when the DUT consists in only the load (neither supply nor losses in wire are considered) or when the load cannot be decoupled from the active part of the circuit and the losses. The aim is then to compute Z_c . Considering the circuit in figure 3.2, it can be written that:

$$Z_m = \frac{V_m}{I_m} = \frac{A_1 V_c + B_1 I_c}{C_1 V_c + D_1 I_c} = \frac{A_1 Z_c + B_1}{C_1 Z_c + D_1}$$

and then

$$Z_c = \frac{\frac{-D_1}{C_1} Z_m + \frac{B_1}{C_1}}{Z_m + \frac{-A_1}{C_1}} = \frac{k_1 Z_m + k_2}{Z_m + k_3} \quad (3.1)$$

This implies that Z_c can be computed from the measure of Z_m and the ABCD parameters representation of the inductive probe. Even without knowing the values of these parameters, the computation can be carried by previously making three characterization measurements with the inductive probe and three different known impedances Z_1 , Z_2 and Z_3 . The measurements are taken in the way it is shown in figure 3.3 and Z_{m1} , Z_{m2} and Z_{m3} are obtained respectively.

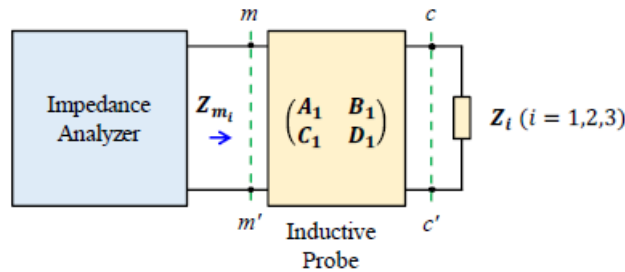


Figure 3.3: Set-up of characterization measurements, taken from [16]

Considering equation (3.1), Z_1 , Z_2 and Z_3 can be expressed in terms of k_1 , k_2 and k_3 and the correspondent measure. Therefore, the three equations can be rearranged into a system with k_1 , k_2 and k_3 as variables:

$$\left. \begin{aligned} Z_1 &= \frac{k_1 Z_{m1} + k_2}{Z_{m1} + k_3} \\ Z_2 &= \frac{k_1 Z_{m2} + k_2}{Z_{m2} + k_3} \\ Z_3 &= \frac{k_1 Z_{m3} + k_2}{Z_{m3} + k_3} \end{aligned} \right\}$$

$$\left. \begin{aligned} k_1 Z_{m1} + k_2 - Z_1 k_3 &= Z_1 Z_{m1} \\ k_1 Z_{m2} + k_2 - Z_2 k_3 &= Z_2 Z_{m2} \\ k_1 Z_{m3} + k_2 - Z_3 k_3 &= Z_3 Z_{m3} \end{aligned} \right\} \Rightarrow \begin{pmatrix} Z_{m1} & 1 & -Z_1 \\ Z_{m2} & 1 & -Z_2 \\ Z_{m3} & 1 & -Z_3 \end{pmatrix} \begin{pmatrix} k_1 \\ k_2 \\ k_3 \end{pmatrix} = \begin{pmatrix} Z_1 Z_{m1} \\ Z_2 Z_{m2} \\ Z_3 Z_{m3} \end{pmatrix}$$

and writing it in vectorial notation

$$\Lambda \vec{k} = \vec{\lambda}$$

Taking into account that $Z_1 \neq Z_2 \neq Z_3$ and assuming $(Z_{m1}, Z_{m2}, Z_{m3})^t$ is not proportional to $(Z_1, Z_2, Z_3)^t$ then Λ has maximum rank and the system is determined. It can be solved by the Cramer's rule getting:

$$\begin{aligned} k_1 &= \frac{\begin{vmatrix} Z_1 Z_{m1} & 1 & -Z_1 \\ Z_2 Z_{m2} & 1 & -Z_2 \\ Z_3 Z_{m3} & 1 & -Z_3 \end{vmatrix}}{\det(\Lambda)} = \frac{\det(\Lambda_1)}{\det(\Lambda)} \\ k_2 &= \frac{\begin{vmatrix} Z_{m1} & Z_1 Z_{m1} & -Z_1 \\ Z_{m2} & Z_2 Z_{m2} & -Z_2 \\ Z_{m3} & Z_3 Z_{m3} & -Z_3 \end{vmatrix}}{\det(\Lambda)} = \frac{\det(\Lambda_2)}{\det(\Lambda)} \\ k_3 &= \frac{\begin{vmatrix} Z_{m1} & 1 & Z_1 Z_{m1} \\ Z_{m2} & 1 & Z_2 Z_{m2} \\ Z_{m3} & 1 & Z_3 Z_{m3} \end{vmatrix}}{\det(\Lambda)} = \frac{\det(\Lambda_3)}{\det(\Lambda)} \end{aligned}$$

and substituting this solution in equation (3.1) it is finally obtained the expression for computing Z_c from the measurement Z_m , and the three characterization measurements and values:

$$Z_c = \frac{\det(\Lambda_2) + \det(\Lambda_1)Z_m}{\det(\Lambda_3) + \det(\Lambda)Z_m} = \frac{a + bZ_m}{c + dZ_m} \quad (3.2)$$

where

$$\begin{aligned} a &= Z_1 Z_2 (Z_{m2} - Z_{m1}) Z_{m3} + Z_1 Z_3 (Z_{m1} - Z_{m3}) Z_{m2} + Z_2 Z_3 (Z_{m3} - Z_{m2}) Z_{m1} \\ b &= -Z_1 Z_2 (Z_{m2} - Z_{m1}) - Z_1 Z_3 (Z_{m1} - Z_{m3}) - Z_2 Z_3 (Z_{m3} - Z_{m2}) \\ c &= Z_1 (Z_{m2} - Z_{m3}) Z_{m1} + Z_2 (Z_{m3} - Z_{m1}) Z_{m2} + Z_3 (Z_{m1} - Z_{m2}) Z_{m3} \\ d &= -Z_1 (Z_{m2} - Z_{m3}) - Z_2 (Z_{m3} - Z_{m1}) - Z_3 (Z_{m1} - Z_{m2}) \end{aligned}$$

3.2 DUT with supply and losses in wire

When the load can be decoupled from the rest of the circuit, then following the figure 3.2 and the two-port circuit theory both representations of the inductive probe and the cable and supply can be combined by multiplying their parameter matrices:

$$\mathbb{T} = \begin{pmatrix} A_1 & B_1 \\ C_1 & D_1 \end{pmatrix} \begin{pmatrix} A_2 & B_2 \\ C_2 & D_2 \end{pmatrix} = \begin{pmatrix} t_{11} & t_{12} \\ t_{21} & t_{22} \end{pmatrix}$$

and therefore, as developed in the previous section:

$$\begin{aligned} Z_m &= \frac{V_m}{I_m} = \frac{t_{11}V_c + t_{12}I_c}{t_{21}V_c + t_{22}I_c} = \frac{t_{11}Z_L + t_{12}}{t_{21}Z_L + t_{22}} \\ Z_L &= \frac{\frac{-t_{22}}{t_{21}}Z_m + \frac{t_{12}}{t_{21}}}{Z_m + \frac{-t_{11}}{t_{21}}} = \frac{h_1Z_m + h_2}{Z_m + h_3} \end{aligned} \quad (3.3)$$

The expression (3.3) allows to compute Z_L from the measure Z_m and the ABCD parameters representation of the inductive probe and the cable and supply. But as in the previous section, this can be achieved without knowing these parameters by taking three pre-characterization measurements and with three different known impedances Z_1 , Z_2 and Z_3 in the way it is illustrated in figure 3.4.

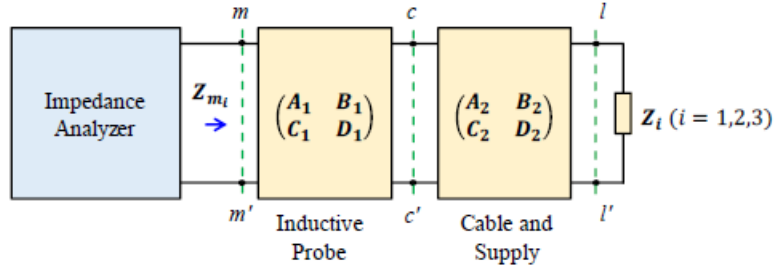


Figure 3.4: Set-up of characterization measurements, taken from [16]

and so again, a system with h_1 , h_2 and h_3 as variables can be written:

$$\left. \begin{aligned} Z_1 &= \frac{h_1Z_{m1} + h_2}{Z_{m1} + h_3} \\ Z_2 &= \frac{h_1Z_{m2} + h_2}{Z_{m2} + h_3} \\ Z_3 &= \frac{h_1Z_{m3} + h_2}{Z_{m3} + h_3} \end{aligned} \right\}$$

$$\begin{pmatrix} Z_{m1} & 1 & -Z_1 \\ Z_{m2} & 1 & -Z_2 \\ Z_{m3} & 1 & -Z_3 \end{pmatrix} \begin{pmatrix} h_1 \\ h_2 \\ h_3 \end{pmatrix} = \begin{pmatrix} Z_1Z_{m1} \\ Z_2Z_{m2} \\ Z_3Z_{m3} \end{pmatrix}$$

$$\Lambda \vec{h} = \vec{\lambda}$$

and making the the same assumptions of the previous section, Cramer's rule can be applied

$$\begin{aligned} h_1 &= \frac{\det(\Lambda_1)}{\det(\Lambda)} \\ h_2 &= \frac{\det(\Lambda_2)}{\det(\Lambda)} \\ h_3 &= \frac{\det(\Lambda_3)}{\det(\Lambda)} \end{aligned}$$

that combined with equation (3.3) gives

$$Z_L = \frac{\det(\Lambda_2) + \det(\Lambda_1)Z_m}{\det(\Lambda_3) + \det(\Lambda)Z_m} = \frac{a + bZ_m}{c + dZ_m} \quad (3.4)$$

where

$$\begin{aligned} a &= Z_1 Z_2 (Z_{m2} - Z_{m1}) Z_{m3} + Z_1 Z_3 (Z_{m1} - Z_{m3}) Z_{m2} + Z_2 Z_3 (Z_{m3} - Z_{m2}) Z_{m1} \\ b &= -Z_1 Z_2 (Z_{m2} - Z_{m1}) - Z_1 Z_3 (Z_{m1} - Z_{m3}) - Z_2 Z_3 (Z_{m3} - Z_{m2}) \\ c &= Z_1 (Z_{m2} - Z_{m3}) Z_{m1} + Z_2 (Z_{m3} - Z_{m1}) Z_{m2} + Z_3 (Z_{m1} - Z_{m2}) Z_{m3} \\ d &= -Z_1 (Z_{m2} - Z_{m3}) - Z_2 (Z_{m3} - Z_{m1}) - Z_3 (Z_{m1} - Z_{m2}) \end{aligned}$$

3.3 Two-probes set-up

The two-probes method has been developed before the single-probe method and it has been used in several articles in the last years [4]. To compare the theoretical robustness and performance of both methods, a Montecarlo and sensitivity analysis have been performed in this work. The schematic and model considered for the two-probes method are the ones used in [16] and shown in the figures 3.5 and 3.6.

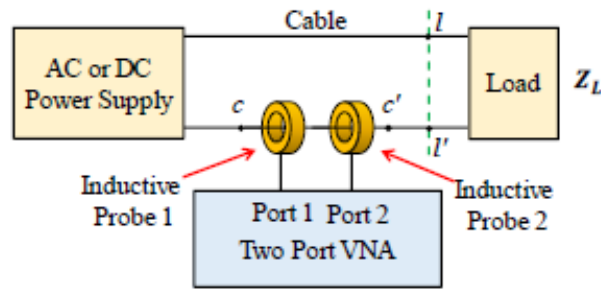


Figure 3.5: Two-probe set-up schematic, taken from [16]

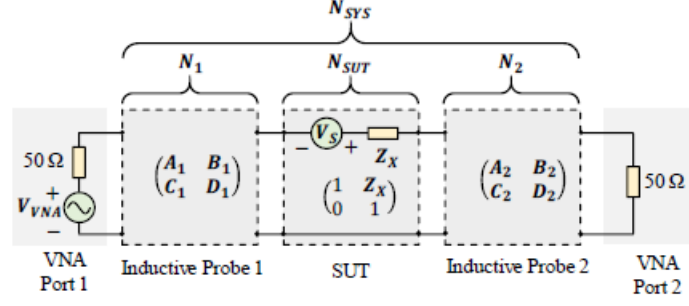


Figure 3.6: Two-probe set-up model, taken from [16]

To address the problem of impedance extraction, a two-port network model approach is adopted. The parameters used are, as in the previous model sections, the ABCD parameters. The blocks N_1 and N_2 represent the ABCD parameters from the inductive probes while N_{SUT} is the representation of the system under test, which has the the following form

$$\begin{pmatrix} v_c \\ i_c \end{pmatrix} = \begin{pmatrix} 1 & Z_x \\ 0 & 1 \end{pmatrix} \begin{pmatrix} v_{c'} \\ i_{c'} \end{pmatrix} + \begin{pmatrix} v_{0c} \\ i_{0c} \end{pmatrix}$$

being v_c , i_c , $v_{c'}$ and $i_{c'}$ the voltage and currents in sections c and c' , respectively, Z_x all the impedances combined from the DUT and v_{0c} and i_{0c} :

$$v_{0c} = v_c \left| \begin{array}{l} v_{c'} = 0 \\ i_{c'} = 0 \end{array} \right. \quad i_{0c} = i_c \left| \begin{array}{l} v_{c'} = 0 \\ i_{c'} = 0 \end{array} \right.$$

as explained in section 2.1.2. When there is no independent source in the DUT the term containing v_{0c} and i_{0c} becomes null and therefore it can be written:

$$N_{SYS} = N_1 * N_{SUT} * N_2$$

$$\begin{pmatrix} A_{sys} & B_{sys} \\ C_{sys} & D_{sys} \end{pmatrix} = \begin{pmatrix} A_1 & B_1 \\ C_1 & D_1 \end{pmatrix} \begin{pmatrix} 1 & Z_x \\ 0 & 1 \end{pmatrix} \begin{pmatrix} A_2 & B_2 \\ C_2 & D_2 \end{pmatrix}$$

Assuming the matrices N_1 and N_2 are not singular, the system equations from above can be solved by pre-multiplying and post-multiplying N_{SYS} by N_1^{-1} and N_2^{-1} , respectively.

$$\begin{pmatrix} 1 & Z_x \\ 0 & 1 \end{pmatrix} = \frac{1}{\det(N_1)\det(N_2)} \begin{pmatrix} D_1 & -B_1 \\ -C_1 & A_1 \end{pmatrix} \begin{pmatrix} A_{sys} & B_{sys} \\ C_{sys} & D_{sys} \end{pmatrix} \begin{pmatrix} D_2 & -B_2 \\ -C_2 & A_2 \end{pmatrix}$$

$$Z_x = \frac{A_2(D_1B_{sys} - B_1D_{sys}) - B_2(D_1A_{sys} - B_1C_{sys})}{(A_1D_1 - B_1C_1)(A_2D_2 - B_2C_2)} \quad (3.5)$$

Then, if losses in wire are taken into consideration and the load Z_L can be decoupled from the system, the impedance value of the load can be extracted by taking another measure $Z_{x'}$ with a known impedance Z_k and subtracting from Z_x the the difference between $Z_{x'}$ and Z_k .

$$Z_L = Z_x - (Z_{x'} - Z_k)$$

3.4 LTSpice implementation of the test set-up

The single-probe method explained previously in the last sections allows, in practice, to extract the impedance value of the load in the DUT by taking only three pre-characterization measures, one measure proper measure with the DUT and then only with this data compute the desired value. Therefore, in simulations the method can be tested using other representations for the inductive probes rather than the ABCD-parameters. Taking this into account, some other models have been considered for the simulations conducted in this work.

The first representation that was used was a pair of coupled coils between the voltage generator and the load, as it can be seen in figure 3.7. The model and values where taken from pages 8-10 of [14] adapted to only one probe instead of two.

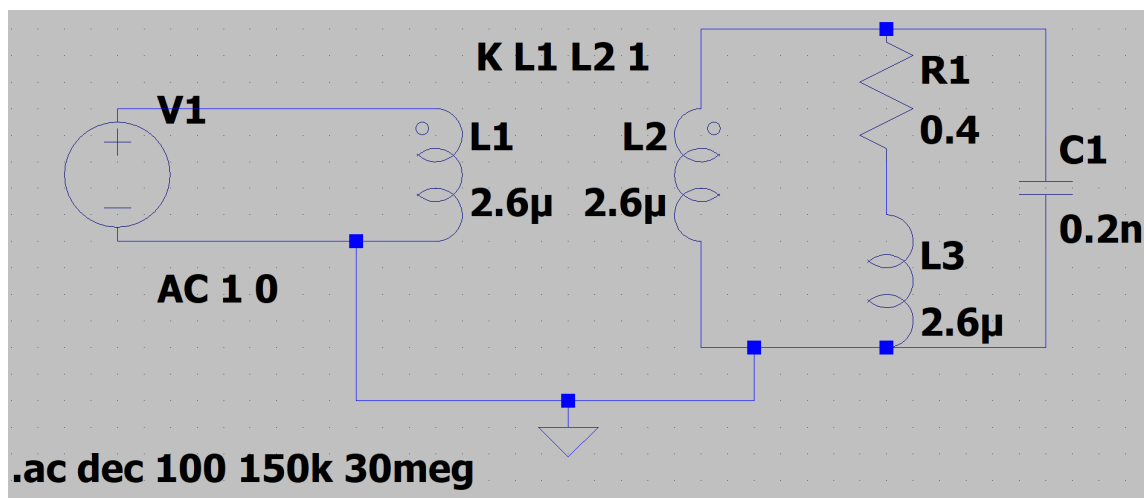


Figure 3.7: Schematic in LTSpice of the coupled coils representing the inductive probe

In order to work similarly as with the other representations, the ABCD parameters are computed.

$$\begin{pmatrix} v_1 \\ v_2 \end{pmatrix} = \begin{pmatrix} L & M \\ M & L \end{pmatrix} \begin{pmatrix} i_1 \\ -i_2 \end{pmatrix} \omega j \quad ; \quad \begin{pmatrix} v_1 \\ i_1 \end{pmatrix} = \begin{pmatrix} A & B \\ C & D \end{pmatrix} \begin{pmatrix} v_2 \\ i_2 \end{pmatrix}$$

$$A = \left(\frac{v_1}{v_2} \right)_{i_2=0} = \frac{L}{M} = 1$$

$$B = \left(\frac{v_1}{i_2} \right)_{v_2=0} = \left(\frac{L^2}{M} - M \right) = 0$$

$$C = \left(\frac{i_1}{v_2} \right)_{i_2=0} = \frac{1}{M\omega j} = 1$$

$$D = \left(\frac{i_1}{i_2} \right)_{v_2=0} = \frac{L}{M} = 1$$

where $L = M = 100$ pH. Currents and voltage references are in figure 3.7.

Also, an ideal transformer representation was used for the inductive probe. The model schematic is shown in figure 3.8. It is ideal in the sense that there are not losses in both the core and the coils, and there is no leakage flux, so all the energy is transmitted and voltages and currents from both sides of the transformer are related through the turns ratio k in the following way:

$$v_1 = kv_2$$

$$i_2 = ki_1$$

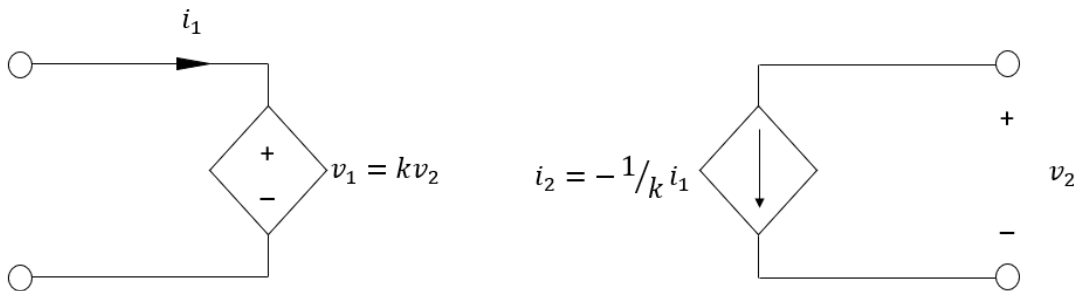


Figure 3.8: Schematic of the ideal transformer representing the inductive probe

Chapter 4

Development of the Work

The work developed in this thesis has focused in simulations of the *single probe method* using several software and scenarios. Also, a Montecarlo and a sensitivity analysis have been carried out with the aim of assessing its theoretical robustness against measurement errors and to compare it to the *double probe method*.

4.1 Parameters and data

The first task conducted was to define the values and configuration of the resistances, inductances and capacitances of a RLC circuit used as a load in the simulations such as its behaviour is similar to one of the loads used in the graphics of page 40 of [16]. A parameters swept was performed with self-developed Matlab scripts and the following values and configuration were selected:

$$\begin{aligned}R &= 0.4\ \Omega \\L &= 2.6\ \mu H \\C &= 0.2\ nF\end{aligned}$$

being R and L in series and both parallel to C.

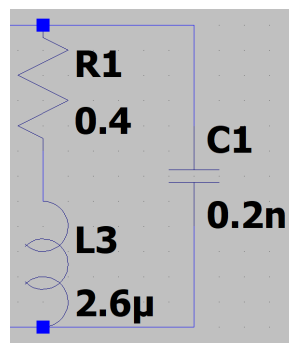


Figure 4.1: Load used in the LTspice models

Additionally, the values for the ABCD parameters of the inductive probe were also defined based on the graphics of page 14 of [16]. A digitization software (Graph Grabber) was used to extract some values of these graphics that would be interpolated later via Matlab (function *interp1* using '*pchip*') for their use. The obtained data is shown in comparative to the original graphic data in figure 4.2.

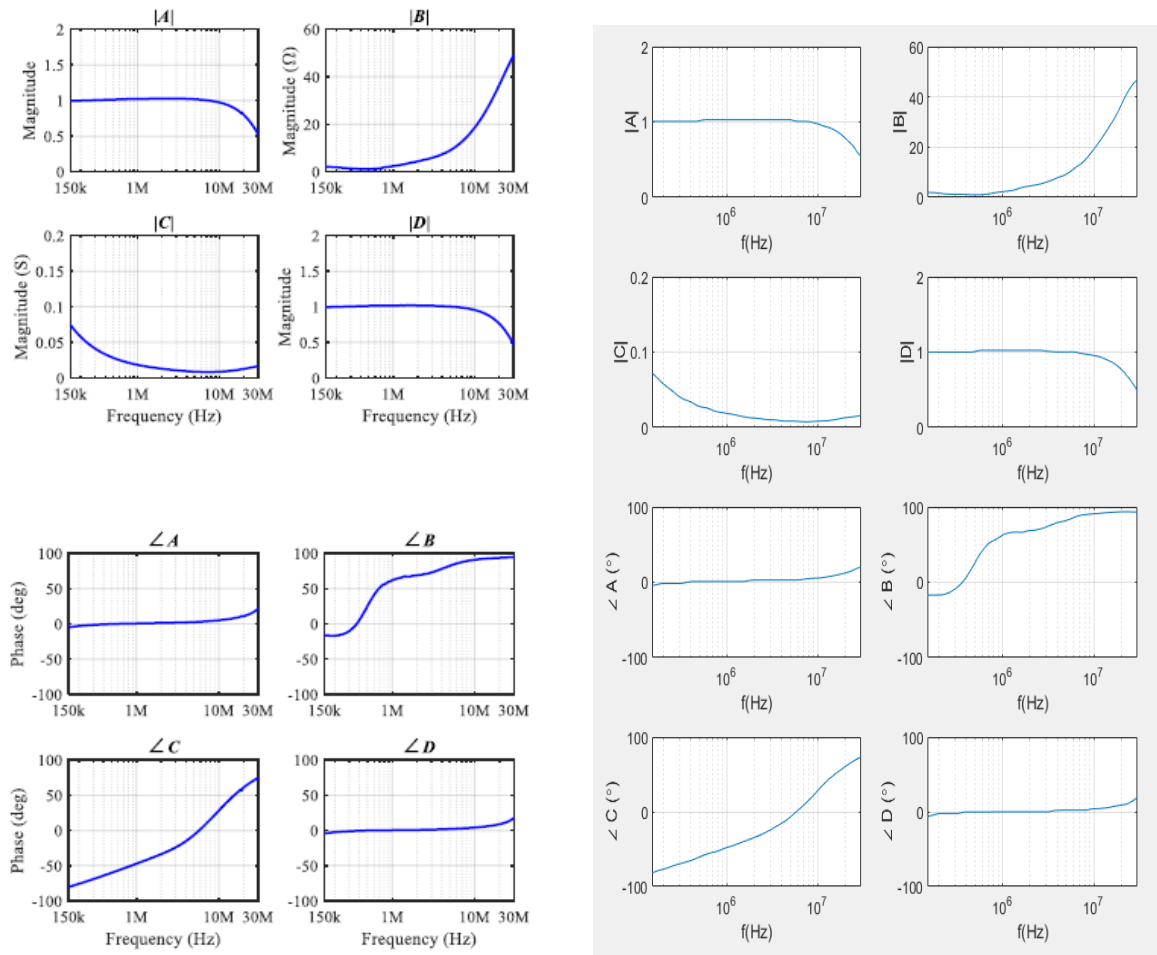


Figure 4.2: Comparative of the original graphic data (left) extracted from [16] and the digitized one (right)

4.2 Matlab simulations

Although in this work the Matlab scripts of this section are being called simulations, they are essentially closer to a mathematical validation test of the method from [16]. The functions used for computation in this section are the ones explained in 4.5.

4.2.1 Ideal passive DUT circuit

The simulation consists in using the equations of 3.1 to compute the impedance value of the RLC load (Z_L) given the values Z_m , Z_{m1} , Z_{m2} and Z_{m3} , those are, the impedance values at the input of the inductive probe (represented by the ABCD parameters extracted from [16]) when the loads are Z_L and three already known impedances, Z_1 , Z_2 and Z_3 , respectively (see figure 3.3). In this simulations this known impedances have been chosen to have the following values: $Z_1 = 0 \Omega$, $Z_2 = 50 \Omega$ and $Z_3 = 1 M\Omega$. With Z_m , Z_{m1} , Z_{m2} and Z_{m3} the value Z_c is computed and compared to the actual impedance value of the load, Z_L . Outcome values are shown in figure 4.3.

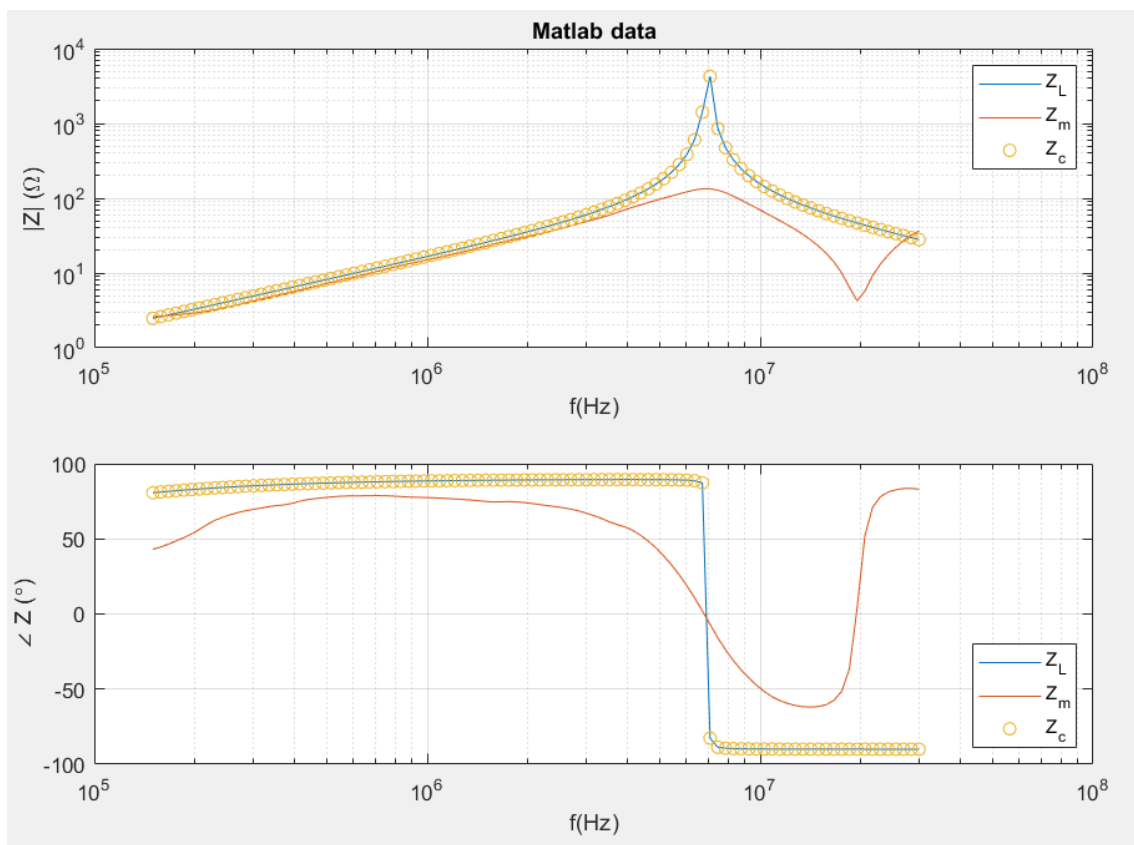


Figure 4.3: Computed values of the simulation

4.2.2 DUT with losses in wire and DC supply

The simulation is essentially the same as the one in the previous subsection but this time the DUT is fed by a 3.7 V battery and losses in the wire are represented by a series impedance $Z_w = 3 \Omega$ (see figure 4.4). The corresponding ABCD parameters of these new components are computed in the way described in section 4.5 and then the same method as the previous subsection is applied to compute Z_c . Also same values are used for Z_L , Z_1 , Z_2 and Z_3 .

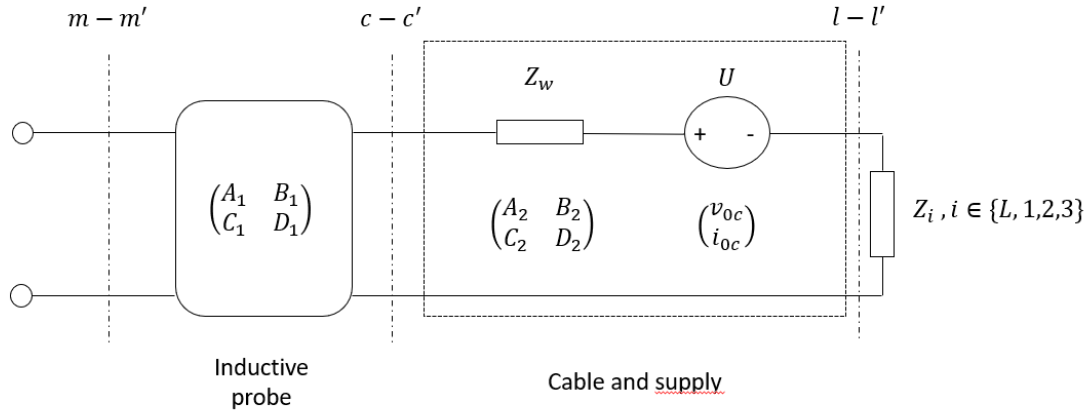


Figure 4.4: Schematic of the simulation

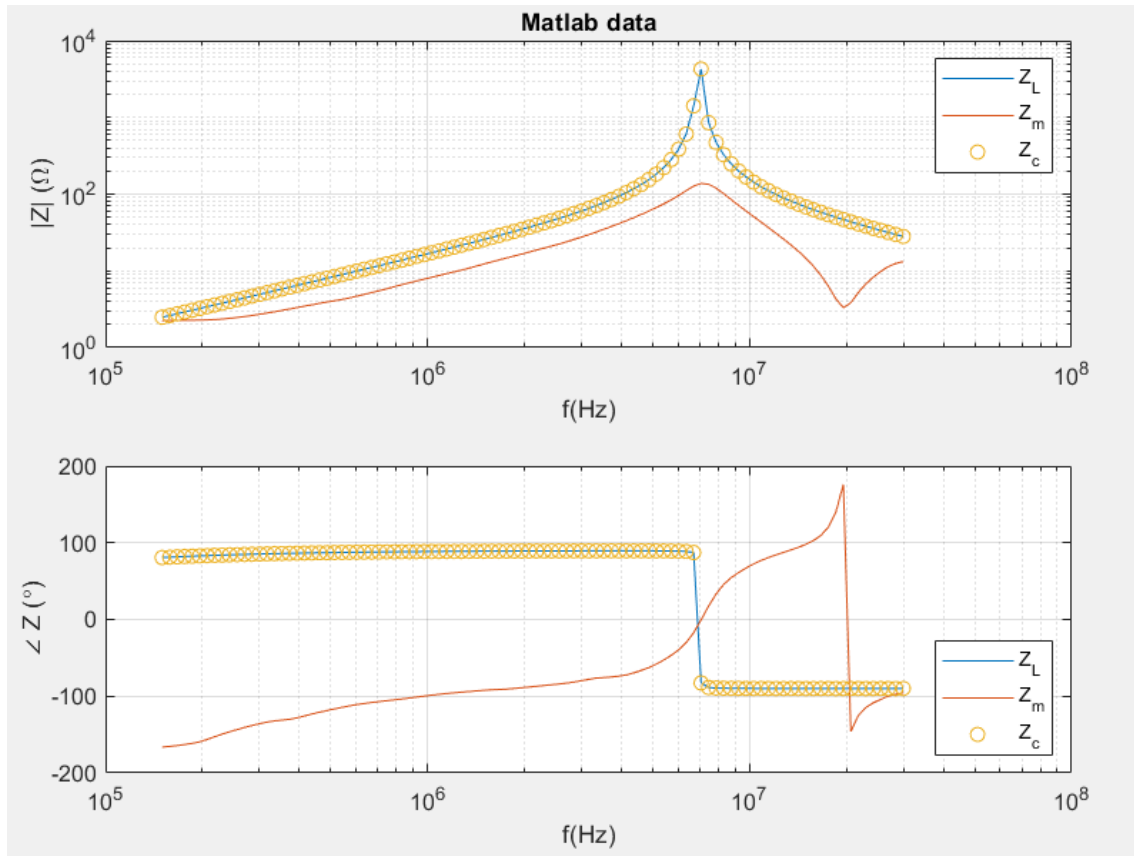


Figure 4.5: Computed values of the simulation

4.3 LTspice and Matlab simulations

In this sections simulations involving the software LTspice are presented. To test the method from [16] 4 simulations have been carried out in AC analysis mode from 150 kHz to 30 MHz. The netlists of these simulations are all like the one in figure 4.6 varying only the load used: one is conducted with the *unknown* load Z_L (figure 4.1) and the other three with the impedances $Z_1 = 0 \Omega$, $Z_2 = 50 \Omega$ and $Z_3 = 1 M\Omega$.

While using this software an important change in the probe representation took place: the ABCD parameters values from [16] could not be loaded so an ideal transformer model was adopted, shown in the figure 3.8. The transmission parameter of this transformer is $K = 0.98$. After the four simulations are done, the outcome data is processed in Matlab following the equations from section 3.1 and Z_c is computed.

```
* C:\Users\pablo\Documents\LTspiceXVII\Draft5.asc
.param pk=0.98
B1 1 0 v='pk * V(2) '
B2 2 0 i='(1/pk) * I(B1) '
R1 2 3 0.4
L1 3 0 2.6u
C1 2 0 0.2n
I1 1 0 ac 1 0
.ac dec 100 150k 30meg
.backanno
.end
```

Figure 4.6: Netlist of the LTspice simulation with the RLC load from figure 4.1.

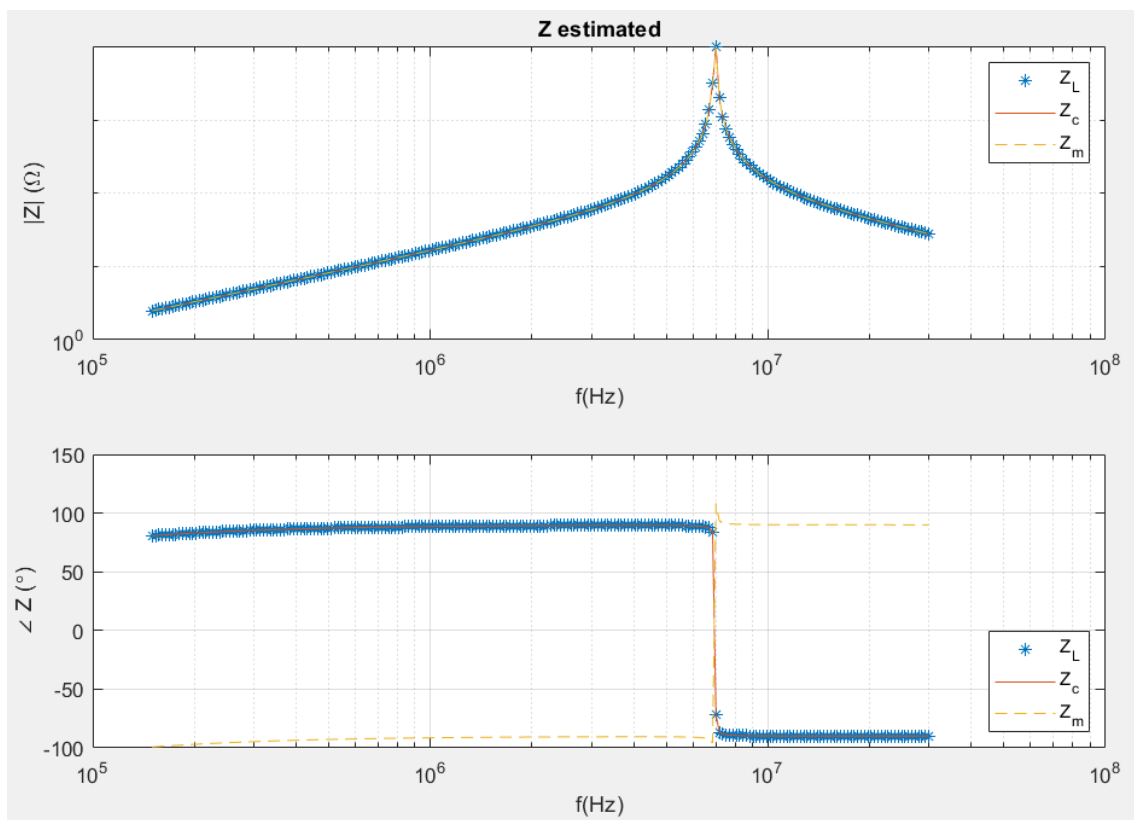


Figure 4.7: Computed values of the simulation

4.4 Qucs and Matlab simulations

In order to use realistic representation of the inductive probe using the ABCD parameters measured from an actual device [16], the software Qucs has been used (further information on [7]). This allowed to load the values of these parameters (which are different for each frequency) in the model and simulate both cases: ideal passive DUT and DUT with battery supply and wire losses.

It must be mentioned that the data of the probe is first prearranged in Matlab in order to create a Touchstone file with the equivalent scattering parameters, which is the only way this software allows to load data from external files. After the simulation the data file generated is read with a Matlab script and the output is processed following the equations of [16].

4.4.1 Ideal passive DUT

In these simulations the only elements that are present are an ideal voltage source, the inductive probe (represented by its scattering parameters) and the DUT, which consists only in the load in this case (see figure 4.8). As in the sections before, four simulations are conducted in AC analysis from 150 kHz to 30 MHz, changing in each one only the load used, which are Z_L (figure 4.1), $Z_1 = 0 \Omega$, $Z_2 = 50 \Omega$ and $Z_3 = 1 M\Omega$. Then the data is exported to Matlab and plotted in the figure 4.9. Again, Z_L is the actual impedance value of the load, Z_m is the impedance at the input of the probe when the DUT is Z_L and Z_c is the impedance computed with the algorithm of section 3.1.

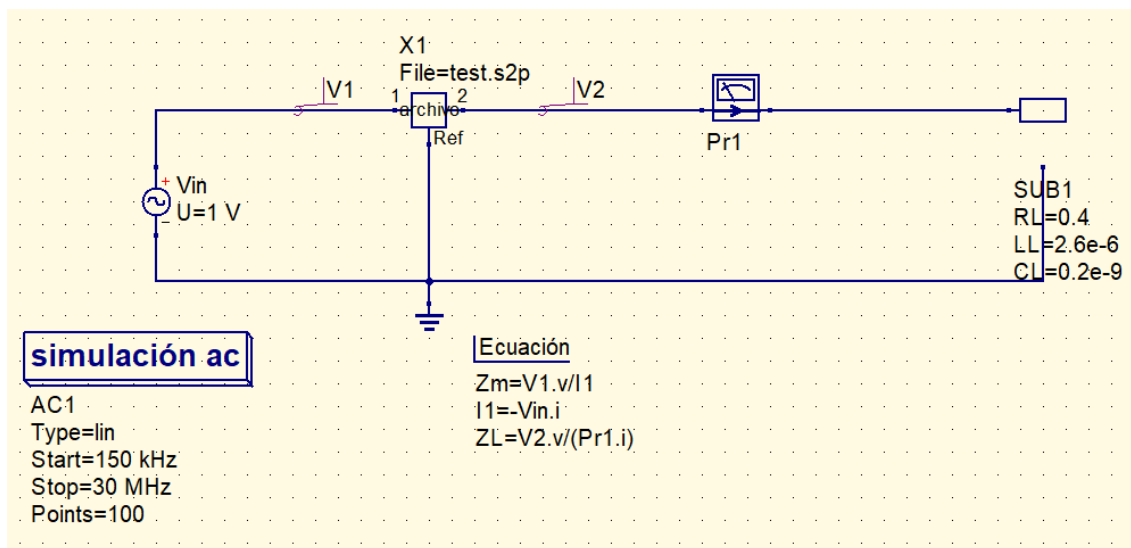


Figure 4.8: View of the Qucs schematics for the simulation with Z_L

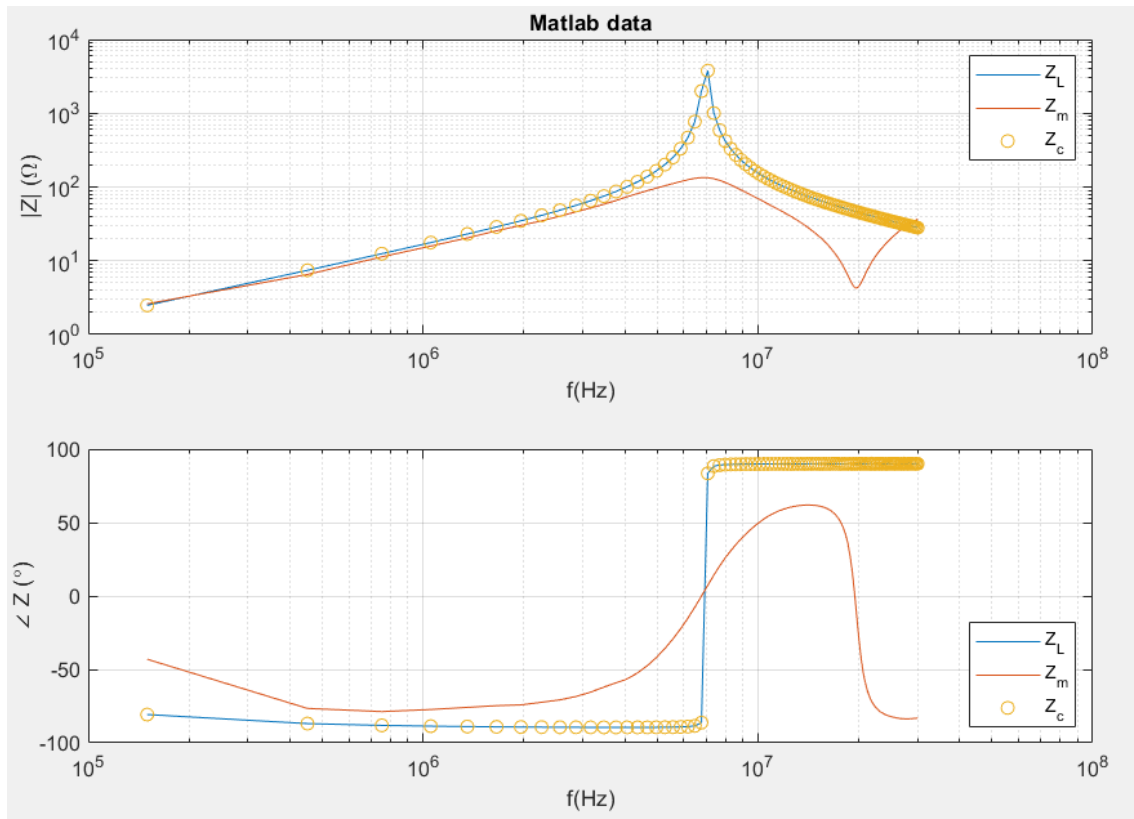


Figure 4.9: Computed values of the simulation

4.4.2 DUT with losses in wire and DC supply

The simulation is performed following the schematic shown in figure 4.10 which is exactly the same as the one in the previous subsection but adding a DC ideal source of 3.7 V in series with an impedance representing the losses in the wire with a value of $Z_w = 3\ \Omega$. Again, four AC simulations are carried out alternating the load among Z_L (figure 4.1), Z_1 ($0\ \Omega$), Z_2 ($50\ \Omega$) and Z_3 ($1\ \text{M}\Omega$), measuring Z_m , Z_{m1} , Z_{m2} and Z_{m3} , respectively. Then the data is processed applying the equations explained in 3.2 via Matlab and the out-coming Z_c (computed value of the load) is plotted against Z_L (actual value of the load) and Z_m (measured value at the probe input) in figure 4.11.

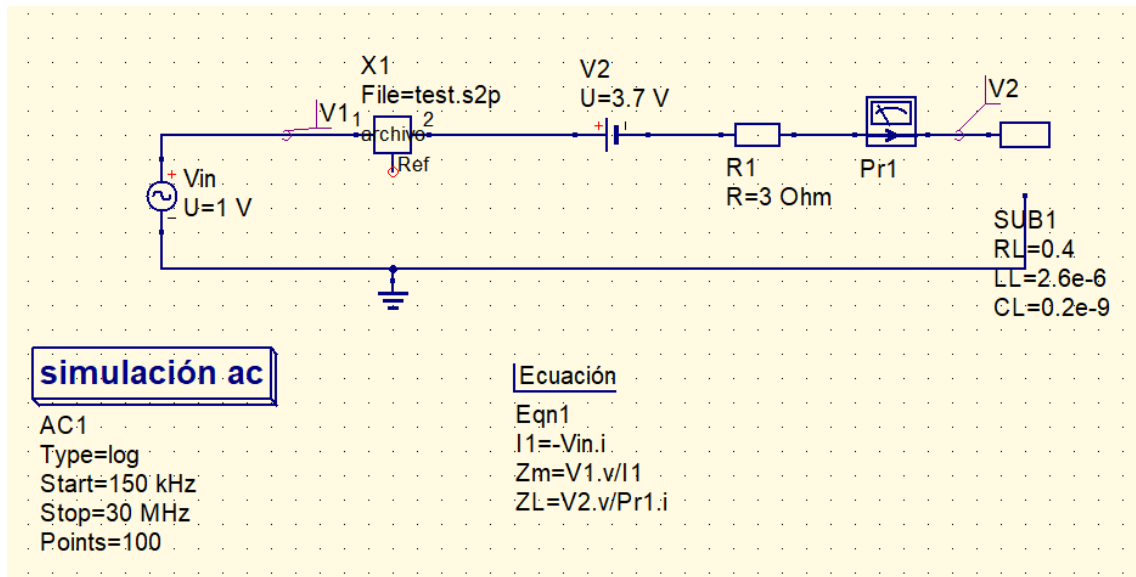


Figure 4.10: View of the Qucs schematics for the simulation with Z_L

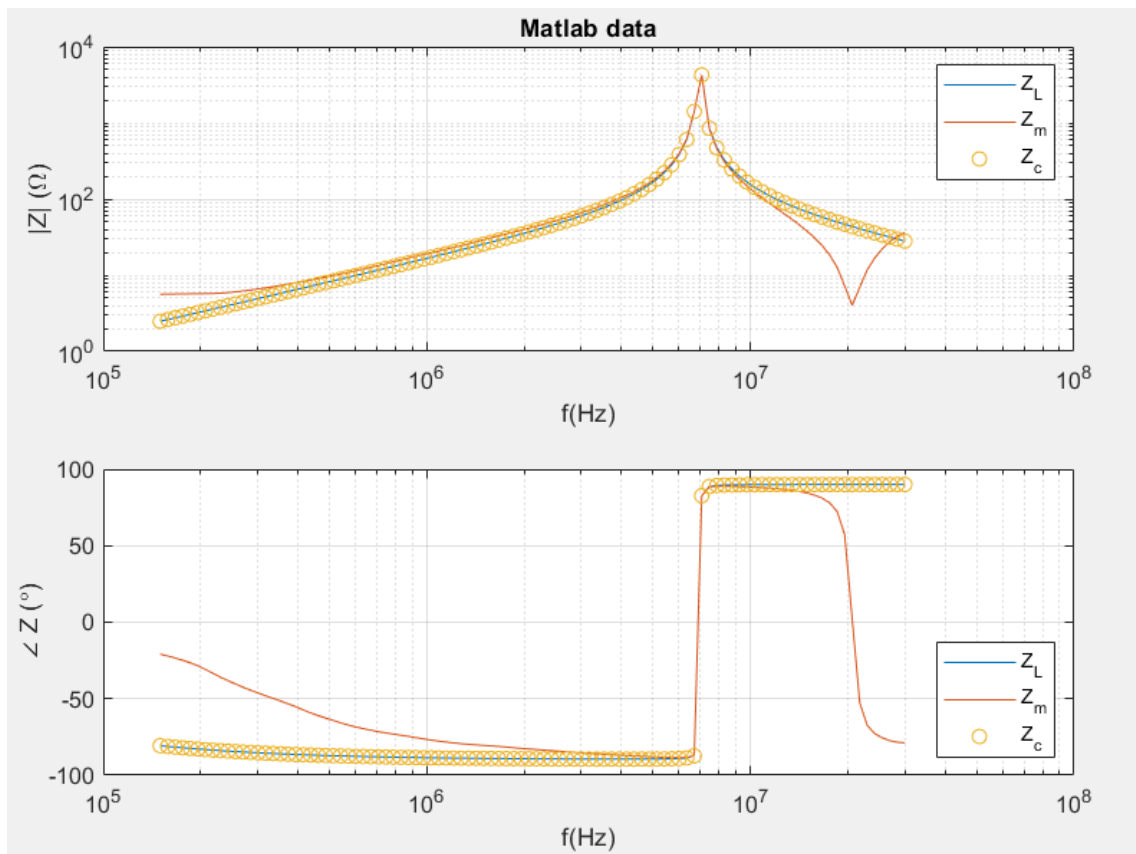


Figure 4.11: Computed values of the simulation

4.5 Montecarlo and sensitivity analysis

4.5.1 Notation

To clarify the notation used in these analysis, the equations of sections 3.1, 3.2 and 3.3 have been rearranged and the functions Γ and Δ are defined. The first one would give the final impedance value Z_c given the parameters of the circuit and the loads Z_L , Z_{m1} , Z_{m2} and Z_{m3} . Instead, the second one would give the impedance measured at the input of the probe Z_{mi} given the circuit parameters and a load Z_i .

Depending on the circuit configuration these functions will have different number of arguments, so it is convenient to add a sub-index to address this matter: 1 is for a passive DUT circuit and 2 is for DUT with DC supply and losses in wire. Then, for the first case functions are defined as it follows:

$$Z_{mi} = \Delta_1(A_1, B_1, C_1, D_1, Z_i) = \frac{A_1 + \frac{B_1}{Z_i}}{C_1 + \frac{D_1}{Z_i}}$$

$$Z_c = \Gamma_1(A_1, B_1, C_1, D_1, Z_1, Z_2, Z_3, Z_m)$$

being A_1 , B_1 , C_1 and D_1 the ABCD parameters of the probe, $i \in \{1, 2, 3, L\}$, Z_1 , Z_2 and Z_3 the pre-characterization impedances and $Z_m = \Delta_1(A_1, B_1, C_1, D_1, Z_L)$, with Z_L being the load impedance. The explicit expression of Γ_1 is the equation (3.2).

When considering DC supply and losses in the wire (second case) new arguments have to be added to the functions. The ABCD parameters representation of these new elements is the one following

$$\begin{pmatrix} v_c \\ i_c \end{pmatrix} = \begin{pmatrix} A_2 & B_2 \\ C_2 & D_2 \end{pmatrix} \begin{pmatrix} v_2 \\ i_2 \end{pmatrix} + \begin{pmatrix} v_{0c} \\ i_{0c} \end{pmatrix}$$

where index c is referring to the output of the probe and index 2, as usually, to the load. A_2 , B_2 , C_2 and D_2 are the ABCD parameters of the losses in wire and v_{0c} and i_{0c} are a consequence of the independent source voltage defined as:

$$v_{0c} = v_c \left| \begin{array}{l} v_2 = 0 \\ i_2 = 0 \end{array} \right. \quad i_{0c} = i_c \left| \begin{array}{l} v_2 = 0 \\ i_2 = 0 \end{array} \right.$$

Consequently, the equations of the whole circuit (that is the voltage source, the probe, the battery, the wire impedance and the load Z_i) can be written as:

$$\begin{pmatrix} v_1 \\ i_1 \end{pmatrix} = \begin{pmatrix} A_1 & B_1 \\ C_1 & D_1 \end{pmatrix} \left[\begin{pmatrix} A_2 & B_2 \\ C_2 & D_2 \end{pmatrix} \begin{pmatrix} v_2 \\ i_2 \end{pmatrix} + \begin{pmatrix} v_{0c} \\ i_{0c} \end{pmatrix} \right]$$

that defining

$$\mathbb{T}_1 = \begin{pmatrix} A_1 & B_1 \\ C_1 & D_1 \end{pmatrix}, \quad \mathbb{T}_2 = \begin{pmatrix} A_2 & B_2 \\ C_2 & D_2 \end{pmatrix}, \quad \mathbb{T} = \mathbb{T}_1 \mathbb{T}_2 = \begin{pmatrix} t_{11} & t_{12} \\ t_{21} & t_{22} \end{pmatrix}$$

and

$$\begin{pmatrix} v_1^* \\ i_1^* \end{pmatrix} = \begin{pmatrix} v_1 \\ i_1 \end{pmatrix} - \mathbb{T}_1 \begin{pmatrix} v_{0c} \\ i_{0c} \end{pmatrix}$$

can be rearranged as

$$\begin{pmatrix} v_1^* \\ i_1^* \end{pmatrix} = \mathbb{T} \begin{pmatrix} v_2 \\ i_2 \end{pmatrix}$$

Now that his equations are similar to the ideal passive DUT case it can be defined $Z_m^* = v_1^*/i_1^* = \Delta_1(t_{11}, t_{12}, t_{21}, t_{22}, Z_i)$ and then, applying the definition of v_1^* and i_1^* , the function Δ_2 is obtained:

$$\begin{aligned} Z_{mi} &= \Delta_2(A_1, B_1, C_1, D_1, A_2, B_2, C_2, D_2, v_1, v_{0c}, i_{0c}, Z_i) = \\ &= \frac{v_1 \Delta_1(t_{11}, t_{12}, t_{21}, t_{22}, Z_i)}{v_1 - A_1 v_{0c} - B_1 i_{0c} + (C_1 v_{0c} + D_1 i_{0c}) \Delta_1(t_{11}, t_{12}, t_{21}, t_{22}, Z_i)} \end{aligned}$$

where Z_i can be either Z_1 , Z_2 , Z_3 or Z_L . As for the Γ_2 expression, the explicit formula is the equation (3.4).

$$Z_c = \Gamma_2(A_1, B_1, C_1, D_1, A_2, B_2, C_2, D_2, v_1, v_{0c}, i_{0c}, Z_1, Z_2, Z_3, Z_m)$$

Apart from these functions, it can be defined Γ_3 for the two-probe set-up case, whose explicit expression is the equation (3.5).

$$Z_c = \Gamma_3(A_1, B_1, C_1, D_1, A_2, B_2, C_2, D_2, A_{sys}, B_{sys}, C_{sys}, D_{sys})$$

4.5.2 Montecarlo analysis

The analysis consists in performing a high number of simulations n_{mont} slightly randomly changing the arguments values of the functions Δ and Γ . This variations are quantified with a parameter that represents the maximum percentage of the nominal values of the variables in which they could be modified. This parameter is called t_{error} .

4.5.2.1 Ideal passive DUT

This analysis is useful to assess the mathematical robustness of the method against measurement errors in practice. The next example have been carried out under the hypothesis of the passive ideal DUT scenario within and a frequency range of 150k-30M Hz. Parameters of the analysis are $n_{mont} = 1000$, $t_{error} = 5\%$, except for Z_2 , whose t_{error} is 10%, and Z_1 and Z_3 , which are defined to be in the ranges 10 – 100 m Ω (short-circuit) and 1 – 10 M Ω (open-circuit), respectively. The simulations data is shown in the figure 4.12 and the nominal values used are:

- A_1, B_1, C_1 and D_1 are taken from [16].
- $Z_1 = 55$ m Ω , $Z_2 = 50$ Ω and $Z_3 = 5.5$ M Ω .
- Z_L is the one in figure 4.1.
- $Z_m = \Delta_1(A_1, B_1, C_1, D_1, Z_L)$

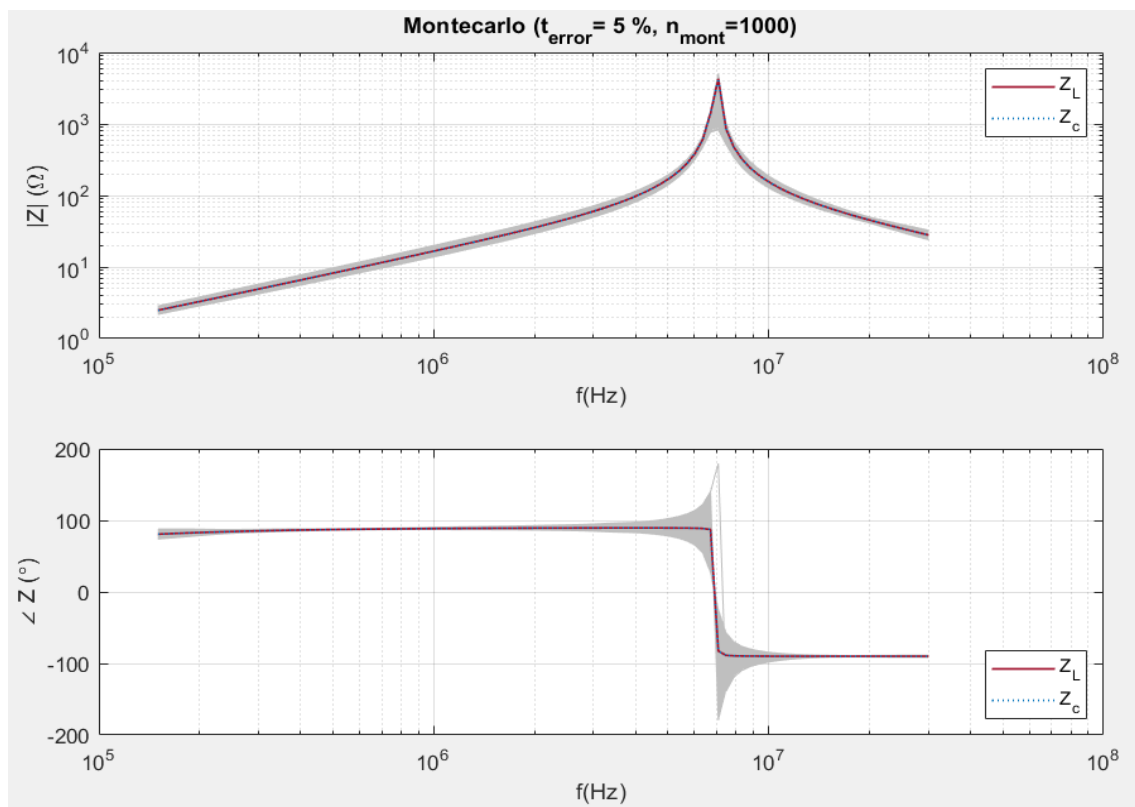


Figure 4.12: Analysis outcome ($n_{mont} = 1000$, $t_{error} = 5\%$)

4.5.2.2 DUT with wire losses and DC supply

Another Montecarlo analysis has been conducted exactly like the one above adding to the circuit a battery supply with a DC voltage of $U = 3.7$ V and wire resistance of $Z_w = 3\ \Omega$. The outcome is shown in figure 4.13 the new nominal values are:

- A_1, B_1, C_1 and D_1 are taken from [16].
- $A_2 = 1, B_2 = Z_w, C_2 = 0$ and $D_2 = 1$.
- $v_1 = 1$ V.
- $v_{0c} = U$ and $i_{0c} = 0$.
- $Z_1 = 55\ \text{m}\Omega, Z_2 = 50\ \Omega$ and $Z_3 = 5.5\ \text{M}\Omega$.
- Z_L is the one in figure 4.1.
- $Z_m = \Delta_1(A_1, B_1, C_1, D_1, Z_L)$

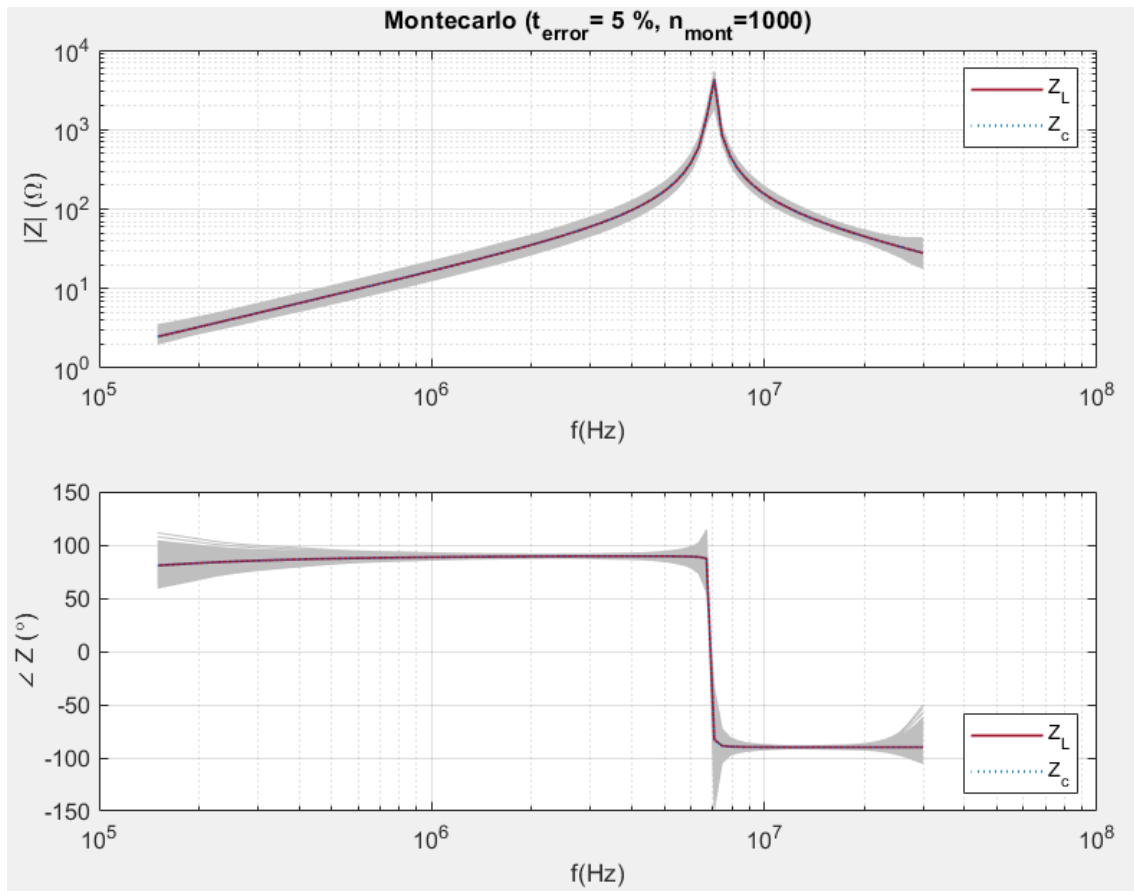


Figure 4.13: Analysis outcome ($n_{mont} = 1000, t_{error} = 5\%$)

4.5.2.3 Two-probes set-up

Following the same procedure as with the single-probe method, it has been performed a Montecarlo analysis for the two-probes method too, within a frequency range of 150k-30M Hz and setting $n_{mont} = 1000$ and $t_{error} = 5\%$. The outcome is shown in figure 4.14 and the nominal values used for the analysis are:

- A_1, B_1, C_1 and D_1 are taken from [16].
- A_2, B_2, C_2 and D_2 are chosen to be exactly the same as the other probe.
- Z_L is the one in figure 4.1.
- $A_{sys}, B_{sys}, C_{sys}$ and D_{sys} are computed by multiplying the matrices N_1, N_{SUT} and N_2 , in that order (see section 3.3).

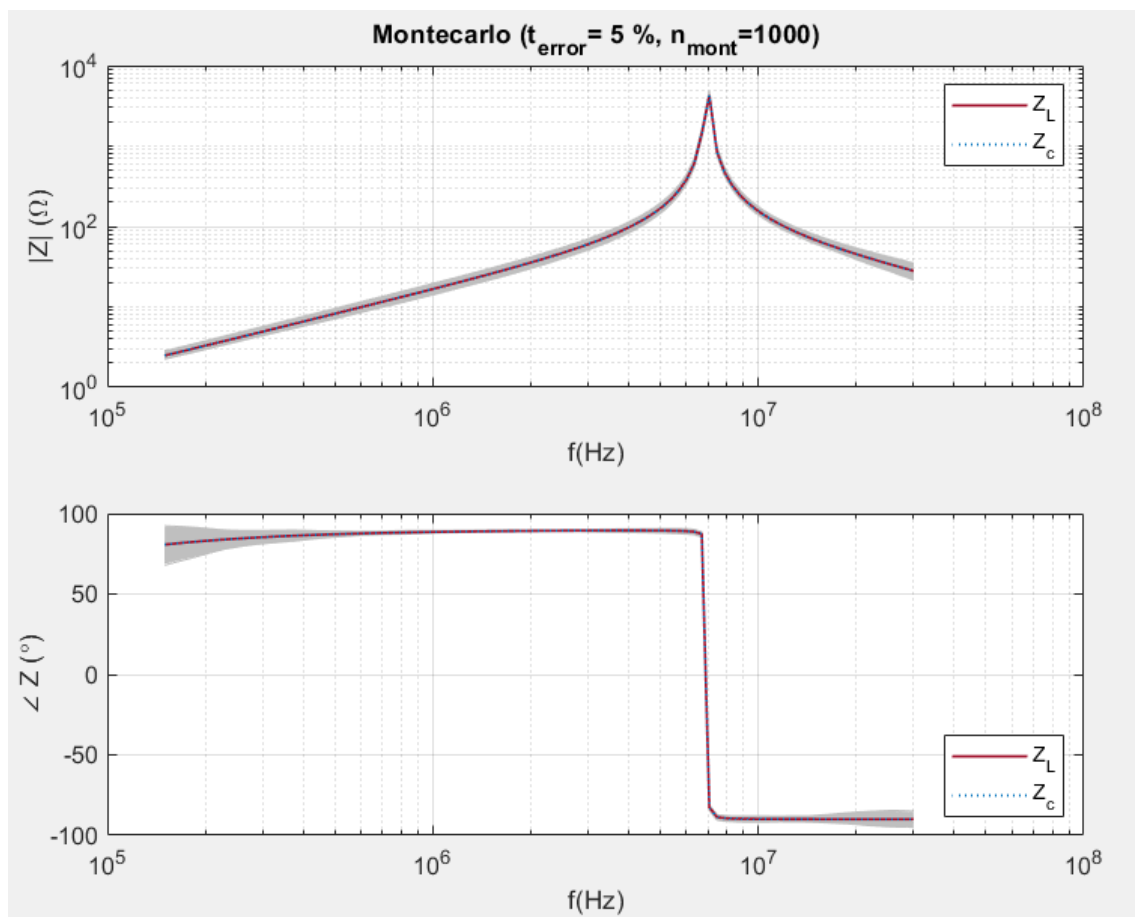


Figure 4.14: Analysis outcome ($n_{mont} = 1000, t_{error} = 5\%$)

4.5.3 Sensitivity analysis

The analysis consists in differentiate the function Γ with respect all its arguments an then normalize with the aim of finding which ones have the most significant impact in the final outcome when they are slightly modified and which ones have less impact in this case. That is, compute the analytical expression of the elasticity of the function Γ :

$$s_x = \frac{\left. \frac{\partial \Gamma}{\partial x} \right|_{\hat{x}}}{\frac{\Gamma}{\hat{x}}}, \quad \forall x \in X$$

being $X = \{A_1, B_1, C_1, D_1, Z_1, Z_2, Z_3, Z_m\}$ in case the analysis is for Γ_1 or $X = \{A_1, B_1, C_1, D_1, A_2, B_2, C_2, D_2, v_1, v_{0c}, i_{0c}, Z_1, Z_2, Z_3, Z_m\}$ in case is for Γ_2 . The symbol $\hat{\cdot}$ denotes nominal values.

A discrete approach of this concept has been considered in this work due to the complex nature of the analytical expressions of Γ_1 and Γ_2 . The main interest is to find what is the impact of a little variation ϵ in the nominal value of the argument $x \in X$ in the variation δ of the Γ function image γ :

$$\begin{aligned} x &= \hat{x}(1 + \epsilon) = \hat{x} + \Delta x \\ &\Downarrow \\ \gamma &= \hat{\gamma}(1 + \delta) = \hat{\gamma} + \Delta \gamma \end{aligned}$$

and applying the discrete definition for the elasticity the wanted ratio is obtained.

$$s_x = \frac{\frac{\Delta \gamma}{\hat{\gamma}}}{\frac{\Delta x}{\hat{x}}} = \frac{\Delta \gamma \hat{x}}{\Delta x \hat{\gamma}} = \frac{\delta}{\epsilon}$$

As an example let the function f be defined as $f(x_1, x_2) = x_1 x_2$, $x_1, x_2 \in \mathbb{R}$ and the nominal values $\hat{x}_1 = 1$ and $\hat{x}_2 = 1$. The correspondent elasticity functions s_{x_1} and s_{x_2} are the ones in figure 4.15. As expected, both are the same because of the equality of the partial derivatives and the interpretation would be that if \hat{x}_1 or \hat{x}_2 are modified in, for example, 1% ($\epsilon = 0.01$) then the value of the function f gets modified in 1% ($\delta = s_{x_1} \epsilon = 0.01$) too.

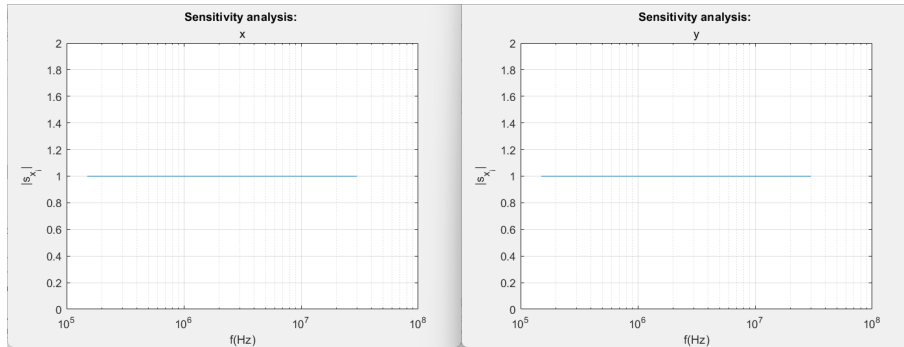


Figure 4.15: Elasticity functions of x and y

4.5.3.1 Ideal passive DUT

For the ideal passive DUT case, that is Γ_1 , the correspondent expressions have been found and plotted in figure 4.16 for a frequency range of 150k-30M Hz. The nominal values used are

- A_1, B_1, C_1 and D_1 are taken from [16].
- $Z_1 = 1 \text{ p}\Omega$, $Z_2 = 50 \text{ }\Omega$ and $Z_3 = 1 \text{ M}\Omega$.
- Z_L is the one in figure 4.1.
- $Z_m = \Delta_1(A_1, B_1, C_1, D_1, Z_L)$

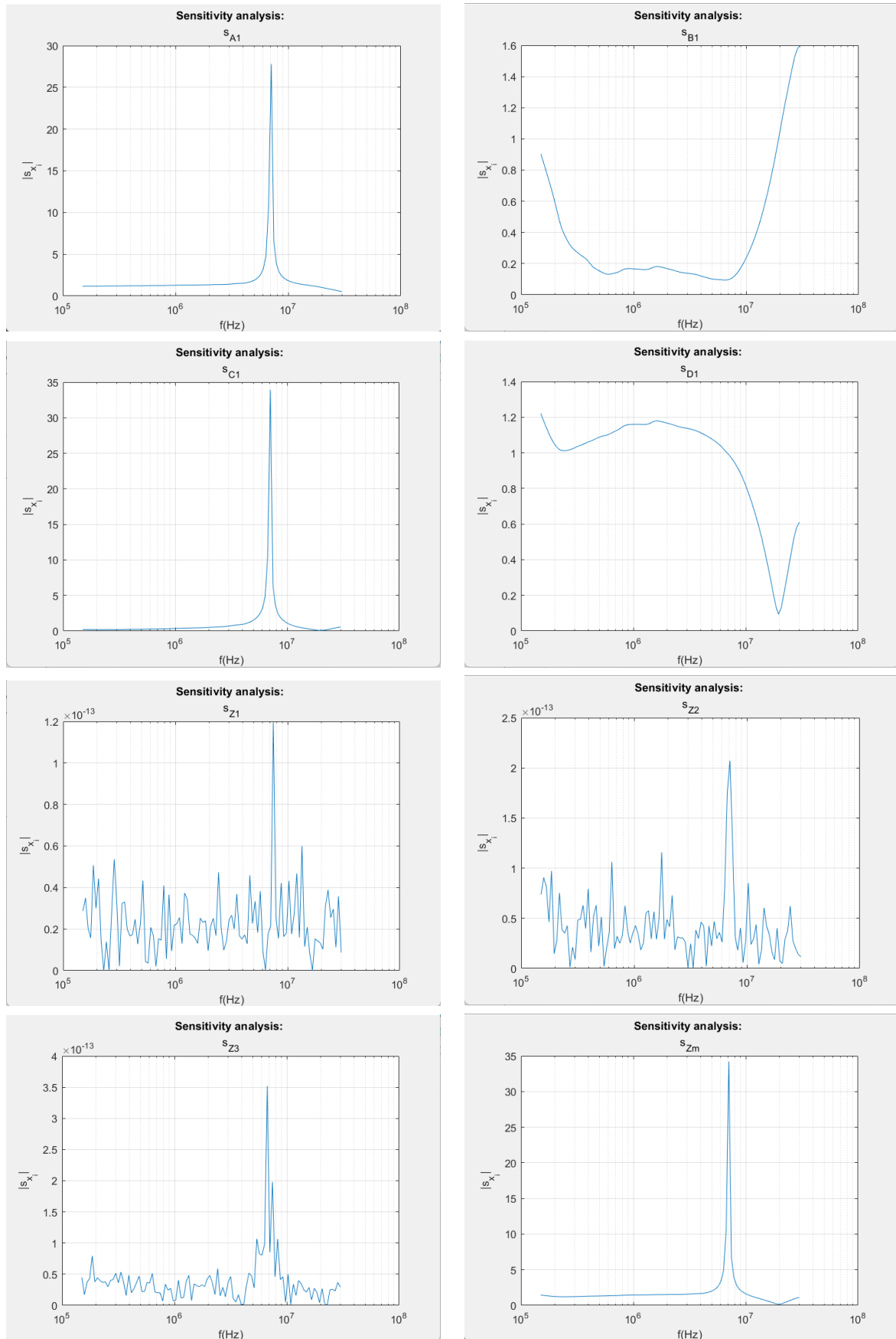


Figure 4.16: Sensitivity analysis outcome

4.5.3.2 DUT with losses in wire and DC supply

For the case of a DUT with a DC battery and losses in wire, that is Γ_2 , the correspondent expressions have been found and plotted in figures 4.17, 4.18 and 4.19 for a frequency range of 150k-30M Hz. In this figure the plots of s_{C_1} and $S_{i_{0c}}$ have been excluded due to the fact that their nominal values are null. The other nominal values that have been used are:

- A_1, B_1, C_1 and D_1 are taken from [16].
- $A_2 = 1, B_2 = Z_w, C_2 = 0$ and $D_2 = 1$.
- $v_1 = 1$ V.
- $v_{0c} = U$ and $i_{0c} = 0$.
- $Z_1 = 1$ p Ω , $Z_2 = 50$ Ω and $Z_3 = 1$ M Ω .
- Z_L is the one in figure 4.1.
- $Z_m = \Delta_1(A_1, B_1, C_1, D_1, Z_L)$

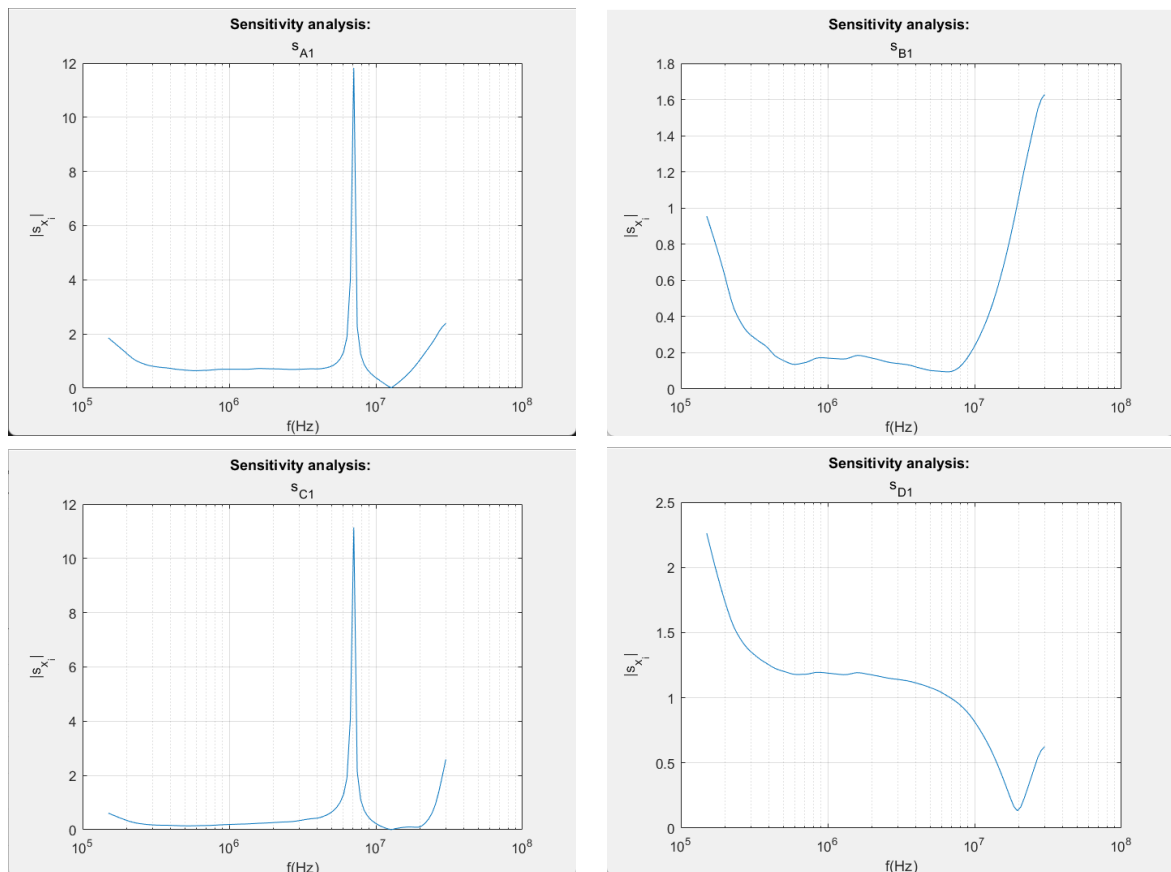


Figure 4.17: Sensitivity analysis outcome

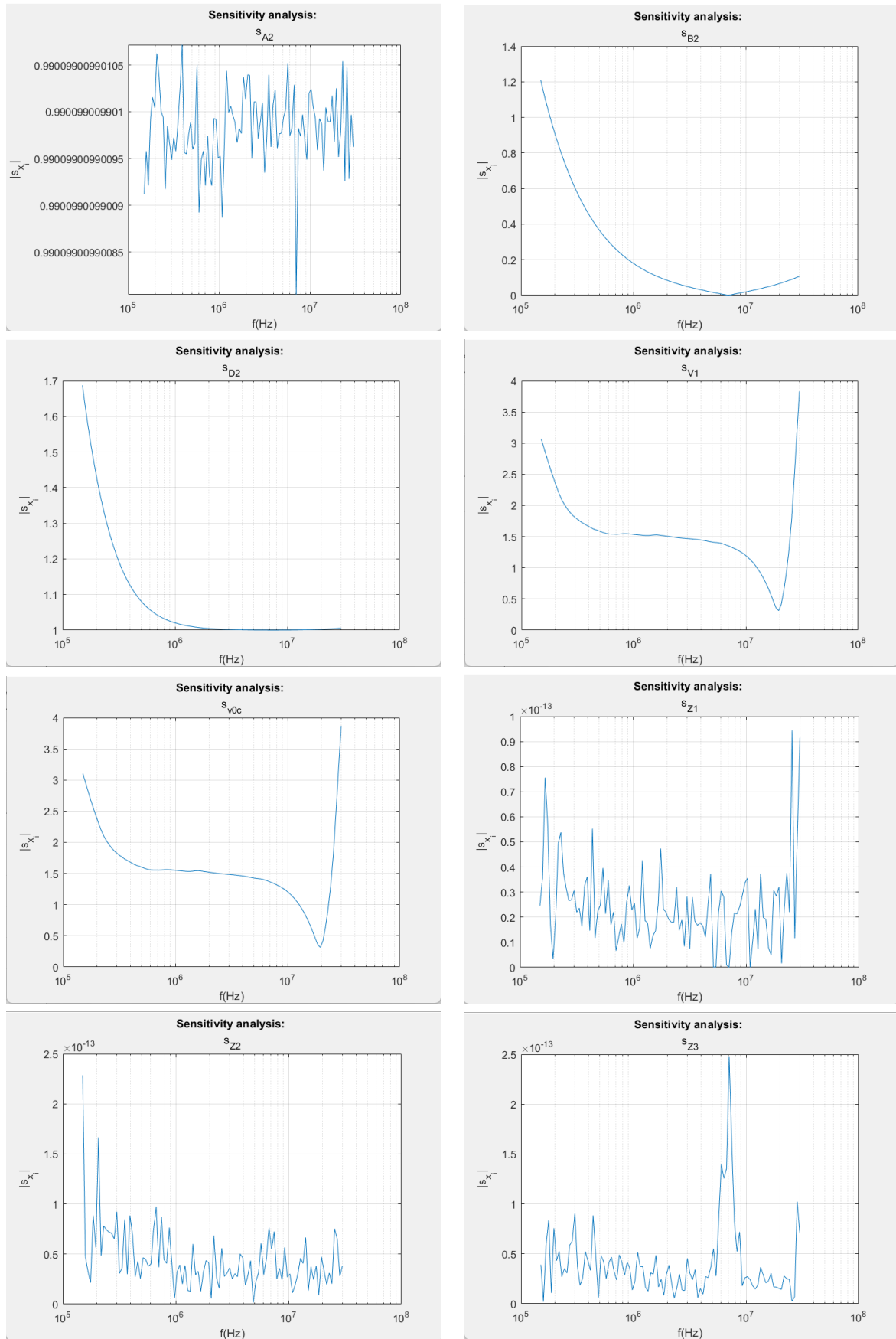


Figure 4.18: Sensitivity analysis outcome

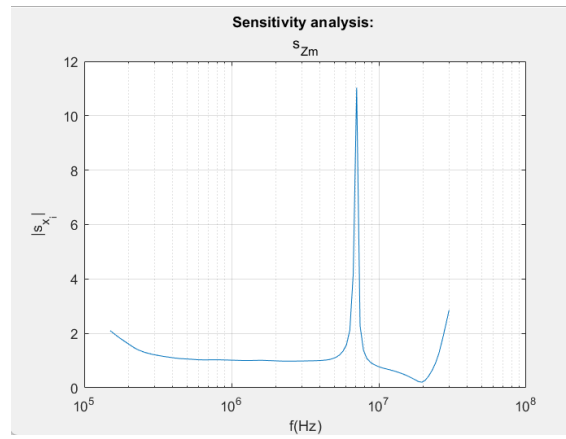


Figure 4.19: Sensitivity analysis outcome

4.5.3.3 Two-probes set-up

For the function Γ_3 , that is, the double-probe method, the analysis has been conducted in the same way as the previous and again, in a frequency range of 150k-30M Hz. The outcome can be seen in figures 4.20 and 4.21 and the nominal values used are

- A_1, B_1, C_1 and D_1 are taken from [16].
- A_2, B_2, C_2 and D_2 are chosen to be exactly the same as the other probe.
- Z_L is the one in figure 4.1.
- $A_{sys}, B_{sys}, C_{sys}$ and D_{sys} are computed by multiplying the matrices N_1, N_{SUT} and N_2 , in that order (see section 3.3).

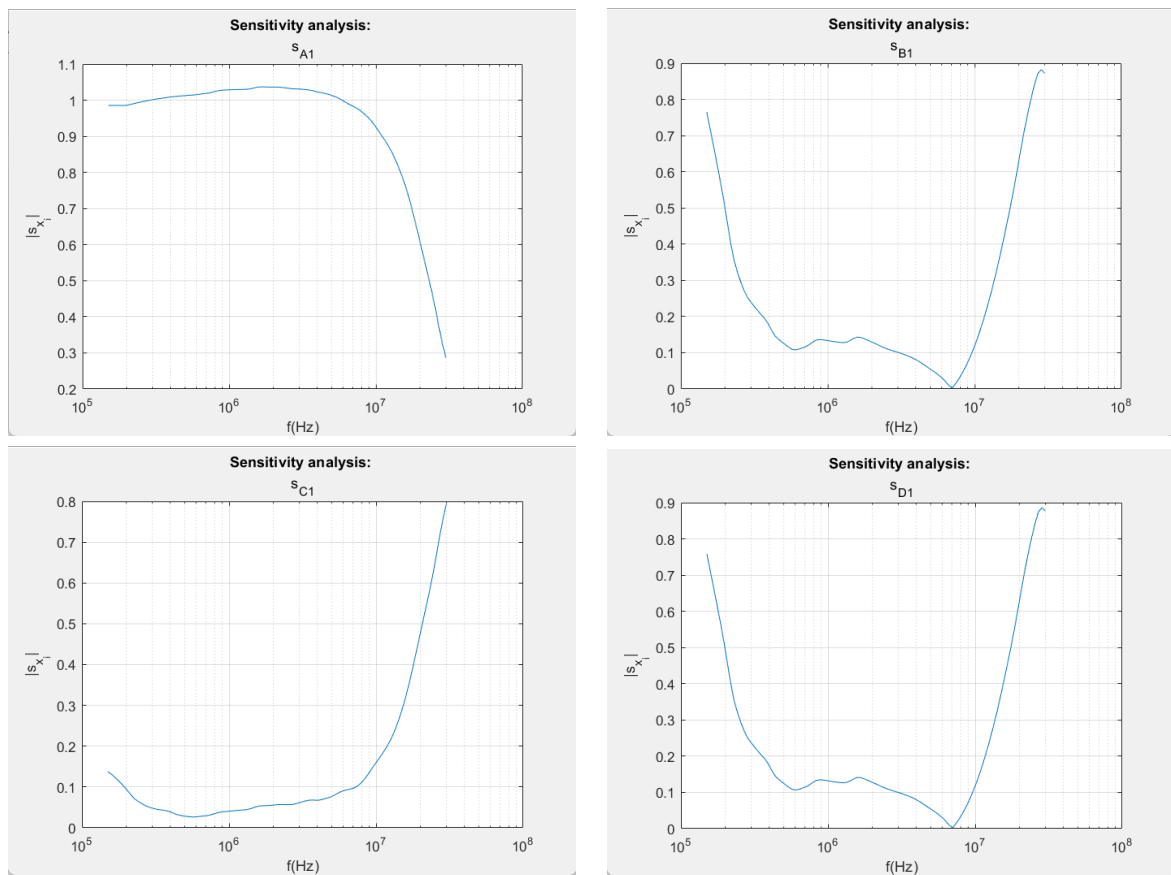


Figure 4.20: Sensitivity analysis outcome

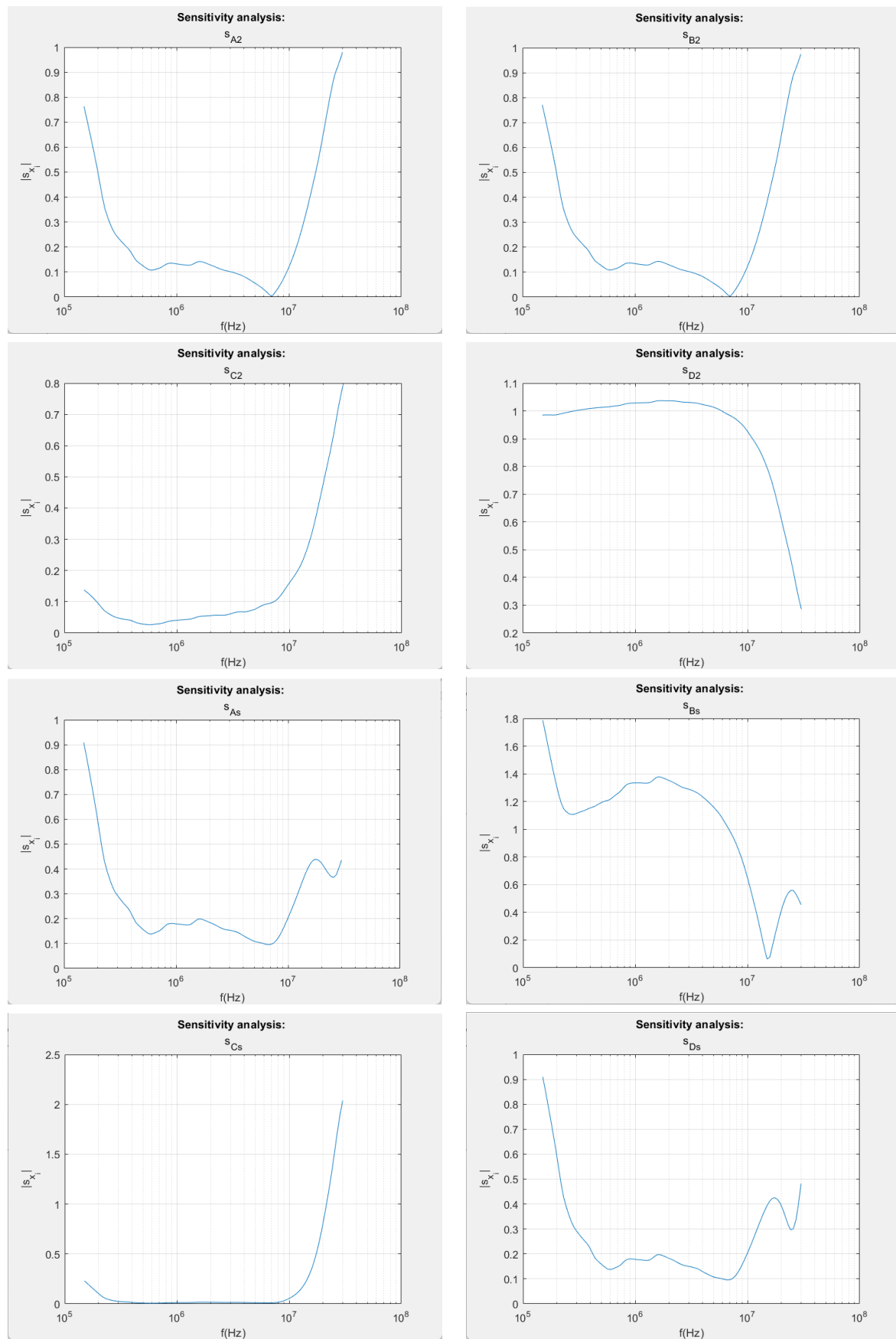


Figure 4.21: Sensitivity analysis outcome

Chapter 5

Remarks and conclusions

5.1 Outcome discussion

5.1.1 Simulations results

As expected, the implementation of the method in the diverse software used has been successful and the target impedance values have been computed correctly under all the representations used.

The LTspice simulation, in which the inductive probe is represented by an ideal transformer model, shows the same accuracy as the Matlab tests with the ABCD-parameters. Also the Qucs simulations, that use S-parameters representation, have the same outcome as the ideal tests performed in Matlab. These results make sense because the single-probe method, in practice, needs only the values of the pre-characterization impedance and the four measurements required for computing the load impedance value, being independent of the representations adopted for the probe or the power system.

5.1.2 Montecarlo analysis results

From the graphics it can be observed that the width of the band obtained is thinner in the case of the two-probes set-up than in the others, for both magnitude and phase and specially in the frequencies near the resonance. This implies that, theoretically, if only the features of the models explained in 3.1, 3.2 and 3.3 are taken into consideration the two-probes set-up seems to be more robust against error in the parameters.

It has to be remarked that the parameters being used for the analysis of the single probe method are more than the ones used in practice (all the parameters related with the representation of the probe, cable and supply for the simulations are not used in practice), therefore it is convenient to know which parameters are causing the largest deviations by inspecting the sensitivity analysis outcome.

5.1.3 Sensitivity analysis results

In accordance with the Montecarlo analysis, the sensitivity analysis shows that the most significant deviations occur in the frequencies near the resonance peak in the case of the single probe method. These sensitivity peaks show up in the parameters A_1 , C_1 and Z_m , and their values are 27.8%, 33.94% and 34.22% for the ideal passive DUT case and 11.82%, 11.14% and 11.03% for the DUT with DC supply and losses in wire case, respectively.

Alternatively, the results of the analysis for the two-probes set-up method are much more homogeneous, always under the value of 2% and without any special response in the resonance. However, in this method all the parameters are measured in practice, whereas in the single probe method the only parameters required in practice are Z_1 , Z_2 , Z_3 and Z_m . Considering that the sensitivity of the three first parameters is almost null, it can be inferred that the only weak point of the single probe method with respect to the double probe method is when the parameter Z_m is measured incorrectly in the frequencies near the resonance of the load.

5.2 Conclusions

The conclusions of this work are presented referring the goals proposed in section 1.2:

- The single probe method has been proven to work correctly in several scenarios and using diverse representations and models for the simulations, as well as its accuracy has been the same in every case.
- The Montecarlo and sensitivity analysis are coherent in the outcome and the most significant deviations of the values computed with the single probe method occur in the frequencies near the electrical resonance of the load, specifically when the parameters A_1 , C_1 and Z_m are modified. On the contrary, the deviations are smaller and more homogeneous in frequency for the double probe method. However, it has to be remarked that A_1 and C_1 are only used in simulations to define a model that represents the reality, therefore in practice the only weaker point of the single probe method with respect to the double probe method is the sensitivity of the parameter Z_m and only in the frequencies mentioned. It must also be considered that these conclusions are valid for the models considered in this work, in which other negative effects for the two-probe set up have not been contemplated, like the probe-to-probe coupling.

5.3 Future works

Finally, a list of suggested future works related to this one is presented:

- Experimental validation of the conclusions of this work.
- Simulations and analysis like the ones performed with other loads and DUTs with different topologies.
- Simulations and analysis like the ones performed as well as experimental validation of the single probe method using time-domain-based instrumentation.
- Comparison of both methods considering other effects present in practical implementations, as for example the probe-to-probe coupling in the double probe method.

Bibliography

- [1] Gyan Ranjan Biswal. *Network theory*. 2017. URL: https://www.vssut.ac.in/lecture_notes/lecture1599051060.pdf.
- [2] M Buzdugan and H Balan. “Hidden schematics of EMI filters”. In: *Renewable Energy and Power Quality Journal (RE&PQJ)* 14 (2016).
- [3] Luca Callegaro. *Electrical impedance: principles, measurement, and applications*. CRC Press, 2012.
- [4] Richard Weng-Yew Chang, Kye-Yak See, and Hu Bo. “In-circuit impedance measurement based on a two-probe approach”. In: *2008 Electrical Design of Advanced Packaging and Systems Symposium*. IEEE. 2008, pp. 35–38.
- [5] David A Howey et al. “Online measurement of battery impedance using motor controller excitation”. In: *IEEE transactions on vehicular technology* 63.6 (2013), pp. 2557–2566.
- [6] Ivan A. Maio. “A Primer on Scattering Parameters”. In: *IEEE* (2008).
- [7] Qucs Team (Michael Margraf and others). *Quite Universal Circuit Simulator*. 2017. URL: <http://qucs.sourceforge.net/docs.html>.
- [8] M.F. Moad. “Two-port networks with independent sources”. In: *Proceedings of the IEEE* 54.7 (1966), pp. 1008–1009. DOI: 10.1109/PROC.1966.4973.
- [9] I. Oganezova et al. “A new and easy approach to create BCI models”. In: *2014 IEEE International Symposium on Electromagnetic Compatibility (EMC)*. 2014, pp. 91–96. DOI: 10.1109/ISEMC.2014.6898949.
- [10] D. Pommerenke, R. Chundru, and S. Chandra. “A new test setup and method for the calibration of current clamps”. In: *IEEE Transactions on Electromagnetic Compatibility* 47.2 (2005), pp. 335–343. DOI: 10.1109/TEMC.2005.847381.
- [11] Steven M Sandler. *Power Integrity: Measuring, Optimizing, and Troubleshooting Power Related Parameters in Electronics Systems*. McGraw-Hill Education, 2014.
- [12] Vuttipon Tarateeraseth. “EMI filter design: Part II: Measurement of noise source impedances”. In: *IEEE Electromagnetic Compatibility Magazine* 1.1 (2012), pp. 42–49.
- [13] Agilent Technologies. *Impedance measurement handbook*. 2009.
- [14] Riccardo Trincherò. “Caratterizzazione di sorgenti di disturbi elettromagnetici con metodo a due pinze”. MA thesis. III Facoltà di Ingegneria, Politecnico di Torino, 2011.

- [15] Arjuna Weerasinghe et al. “In-Circuit Differential-Mode Impedance Extraction at the AC Input of a Motor Drive System”. In: *2021 Asia-Pacific International Symposium on Electromagnetic Compatibility (APEMC)*. IEEE. 2021, pp. 1–4.
- [16] Sudharma Deshapriya Kotuwegedara Harsha Yashoman Arjuna Weerasinghe. “Single probe in-circuit impedance extraction based on inductive coupling approach”. PhD thesis. School of Electrical and Electronic Engineering, Nanyang Technological University, 2021.
- [17] Tomiharu Yamaguchi and Akinori Ueno. “Capacitive-Coupling Impedance Spectroscopy Using a Non-Sinusoidal Oscillator and Discrete-Time Fourier Transform: An Introductory Study”. In: *Sensors* 20.21 (2020). ISSN: 1424-8220. DOI: 10.3390/s20216392. URL: <https://www.mdpi.com/1424-8220/20/21/6392>.
- [18] Zhenyu Zhao et al. “Eliminating the Effect of Probe-to-Probe Coupling in Inductive Coupling Method for In-Circuit Impedance Measurement”. In: *IEEE Transactions on Instrumentation and Measurement* 70 (2021), pp. 1–8. DOI: 10.1109/TIM.2020.3013688.